STUDENT POSTERS

NUCLEAR DAYS 2023

Pilsen, Czech Republic

www.jadernedny.cz

Poster Scientific Committee

doc. Ing. František HEZOUČKÝ, Ph.D.	University of West Bohemia
RNDr. Miroslav KAWALEC	Czech Nuclear Society
Ing. Karel BÍŽA	ÚJV Řež, a. s.
Ing. Josef Královec, CS.	

Organizing Committee

Ing. Jan ZDEBOR, CSc.	University of West Bohemia
Ing. Michal VOLF	University of West Bohemia
Ing. Jana JIŘIČKOVÁ, Ph.D.	University of West Bohemia
Ing. Jiří FRANK	University of West Bohemia
Michaela VACKOVÁ	University of West Bohemia
Lucie GRUSOVÁ	ŠKODA JS a.s.

Partners of Nuclear Days 2023

General partner

Platinum partner

Gold partners

Silver partners

Media partners

Podpořeno

This event has been partially supported by the ENEN2plus project founded by the European Union (HORIZON-EURATOM- 2021-NRT-01-13 101061677).

BACHELOR STUDENTS

VALIDATION OF PROTOTYPE FOR VISCOSITYMEASUREMENT OF MOLTEN CORIUM

Matej Leško

Faculty of Mechanical Engineering, Czech Technical University in Prague

In a severe reactor accident with core meltdown, corium is produced Corium is a lava like mixture of molten nuclear fuel and other materials that it gets in contact with such as fuel rod covering, internal reactor parts or concrete For better modelling of such accidents, it is important to know the properties of the corium, in particular its viscosity, which is very difficult to detect experimentally because of the high temperature of the liquid corium (the melting temperature of UO 2 is approximately 2830 C) One solution to this problem is the use of viscosimeter with rotor made of heat resistant tungsten.

The topic of this work is the experimental verification of the functionality of a viscometer prototype in particular its rotor) designed to measure the viscosity of a molten corium mixture The rotor of the viscometer is planned to be made of difficult to machine tungsten, and therefore a new design in the form of 2 easy to make eccentrically positioned pins was created

Validation of prototype for viscosity measurement of molten corium

Matej Leško, Master's Thesis, 2022
Supervisor: Jan Přehradný, consultant: Jan Štěpánek

Faculty of Mechanical Engineering, Technická 4, 160 00 Prague, Czech Republic
Czech Technical University in Prague
Research Centre Řež, Hlavní 130, 250 68 Husinec-Řež, Czech Republic

matej.lesko@fs.cvut.cz

CTU CZECH TECHNICAL UNIVERSITY IN PRAGUE

CVŘ Research Centre Řež

Introduction

In a severe reactor accident with core meltdown, corium is produced. Corium is a lava like mixture of molten nuclear fuel and other materials that it gets in contact with, such as fuel rod covering, internal reactor parts or concrete. For better modelling of such accidents, it is important to know the properties of the corium, in particular its viscosity, which is very difficult to detect experimentally because of the high temperature of the liquid corium (the melting temperature of UO_2 is approximately 2830 °C). One solution to this problem is the use of viscosimeter with rotor made of heat-resistant tungsten.

The topic of this work is the experimental verification of the functionality of a viscometer prototype (in particular its rotor) designed to measure the viscosity of a molten corium mixture. The rotor of the viscometer is planned to be made of difficult-to-machine tungsten, and therefore a new design in the form of 2 easy-to-make eccentrically positioned pins was created.

Description of the prototype measuring apparatus

A cup with the solution was placed on the heating device, in which the tested rotor of the viscometer was immersed. An electric motor was located on top of the viscometer. The shaft of the electric motor and the shaft of the rotor is connected by a torsion spring allowing the shafts to rotate relative to each other.

A resistive force proportional to the viscosity of the liquid is generated at the rotor pins, which create a moment on the shaft leading from the rotor to the torsion spring. This moment induces a twist on the spring of the observed angle α, proportional to the viscosity of the fluid.

A cut was made in the upper and lower discs and optical sensors were used to monitor the angle α by which the two shafts were rotated relative to each other.

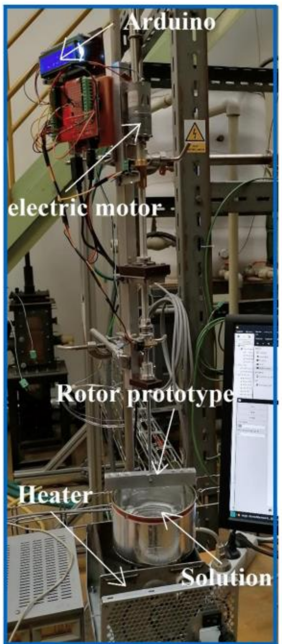

Figure 1: Description of measuring apparatus

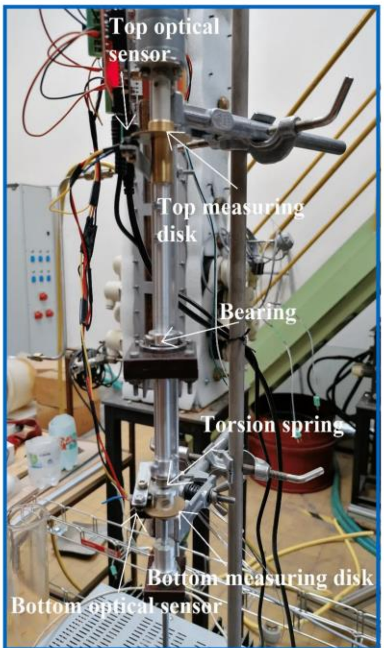

Figure 2: Describtion of viscosimeter prototype

Description of the experiment

Solutions of glycerine and water in different concentrations and sunflower oil were prepared. These solutions were placed on a heating apparatus and their viscosity was measured over a range of temperatures using an industrial viscometer. Theoretical values of the viscosities were also traced, and these data were subsequently compared with the values obtained with the prototype.

The prototype viscometer measured the temperature of the solution and the torsion angle of the torsion spring. A relationship 1.1 between the measured angle and viscosity was derived and then fit in an iterative manner to best replicate the theoretical viscosity values for all solutions. In this way, the values of E = 7,2 $[\frac{rad}{N}]$ a B = -0,35$[\frac{m}{s}]$ were obtained. G is a constant that was calculated as shown in relationship 1.2

$$\mu = \sqrt[B]{\frac{E \cdot G}{\alpha}} \cdot d \cdot \rho \cdot v$$

Equation 1.1 Relationship between viscosity and spring torsion angle

$$G = \frac{\rho \cdot (\pi \cdot n)^2 \cdot r^3 \cdot L \cdot d}{900}$$

Equation 1.2 Description of the constant G

Measurement results

Here is a plot of the coefficient F values as a function of the total relative error of all viscosity measurements using the data measured by prototype from the theoretical values. Also included here are representative plots from measurements of a 50% glycerine water solution at 100 rpm and a 80% glycerine water solution at 102 rpm.

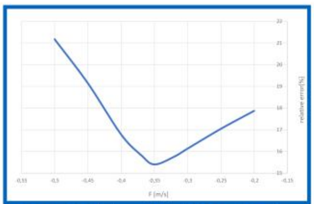

Figure 3 Relative error [%] as a function of constant E [m/s]

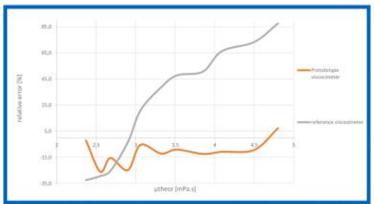

Figure 5 Measurement of relative errors of 50 % glycerine – water solution

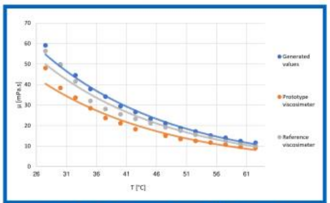

Figure 4 Measurement of 80 % water - glycerine solution at 102 rpm

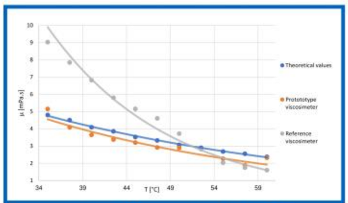

Figure 6 Measurement of 50 % water – glycerine solution at 100 rpm

Conclusion

- 8 measurements of different solutions at different rotary speeds were made.
- It has been shown that viscosity can be measured with this viscometer rotor prototype.
- In some cases, the prototype viscometer measured more accurately than the purchased model.
- As the speed increases, the measurement accuracy of the prototype viscometer decreases because turbulent flow occurs in the solutions due to the increased circumferential velocity of the pins.

References

[1] Didier Jacquemain, Ahmed Bentaïb, Hervé Bonneville, Gérard Cénérino, Bernard Clément, François Corenwinder etc. Nuclear Power Reactor Core Melt Accidents - Current State of Knowledge. France, 2015, IRSN

[2] Koichi Takamura, Herbert Fischer, Norman R. Morrow. Physical properties of aqueous glycerol solutions. Journal of Petroleum Science and Engineering (2012), volume 98-99, page 50-60

[3] Jan Ježek, Blanka Váradiová a Josef Ada. Mechanika Tekutin. Praha, 2000, Vydavatelství ČVUT

QUALITY CONTROL FOR 4D ECTRACRANIAL STEREOTAXIC RADIOTHERAPY TREATMENT GUIDED BY CONE BEAM CT

Marcos Carrilo, Mercedes del Pilar

National University of San Marcos, Peru

The treatment of patients with early-stage lung cancer with surgery is the first choice, and in the medical literature it is described that partial lung resection to treat metastases prolongs survival and may achieve a cure in some patients, but not all patients can benefit from this treatment. The therapeutic options for these medically inoperable patients, then extracranial stereotaxic radiotherapy emerges as an alternative and effective treatment. In order to increase the precision and safety of this technique at the National Institute of Neoplastic Diseases (INEN), extracranial stereotaxic radiotherapy has been implemented through 4D verification guided by Cone Beam, of an Elekta brand Infinity linear accelerator. , which allows, thanks to the XVI 4D System, the acquisition of 4D tomographic images in the accelerator, and in this way monitor the movement of the tumor, defining a maximum amplitude of the movement of the tumor before treatment, thus damaging less healthy lung volume. The objective of this study is to describe the technique of extracranial stereotaxic radiotherapy of lung injury using a 4D verification system.

Quality Control for 4D Ectracranial Stereotaxic Radiotherapy Treatment Guided by Cone Beam CT

[1]Marcos Carrillo , Mercedes del Pilar.
National University of San Marcos, Peru
10130030@unmsm.edu.pe

Introduction

The treatment of patients with early-stage lung cancer with surgery is the first choice, and in the medical literature it is described that partial lung resection to treat metastases prolongs survival and may achieve a cure in some patients, but not all patients can benefit from this treatment [1]. The therapeutic options for these medically inoperable patients, then extracranial stereotaxic radiotherapy emerges as an alternative and effective treatment. In order to increase the precision and safety of this technique at the National Institute of Neoplastic Diseases (INEN), extracranial stereotaxic radiotherapy has been implemented through 4D verification guided by Cone Beam, of an Elekta brand Infinity linear accelerator. , which allows, thanks to the XVI 4D System, the acquisition of 4D tomographic images in the accelerator, and in this way monitor the movement of the tumor, defining a maximum amplitude of the movement of the tumor before treatment, thus damaging less healthy lung volume. The objective of this study is to describe the technique of extracranial stereotaxic radiotherapy of lung injury using a 4D verification system

Methods and Materials

This study describes the treatment and verification of the dose prescribed by the doctor, of a patient with lung injury with this technique in our center. An Elekta brand linear accelerator (Infinity) was removed, as shown in Figure 1, the radiation beam was 6MV and the dosimetric detection system for relative dosimetry was the PTW brand Octavius 4D and it was also used. He also released a software for 3D gamma analysis that was Verisoft (PTW).

During the simulation of this patient, as shown in Figure 2, a four-dimensional computed tomography (4DCT) was acquired to assess intra-fraction changes, the Planning System (PS) used was Monaco v. 5.11. 01 (Elekta), this planner performed the dose calculation using the Monte Carlo (MC) algorithm.

Figure 1. Elekta Infinity Linear Accelerator

Figure 2. Positioning of the patient in the linear accelerator

The planning volume (PTV) was created by giving a 5mm expansion to the internal treatment volume (ITV). The prescribed dose of PTV was 5 fractions of 10 Gy. For treatment planning, the VMAT technique was used, using two round-trip coplanar arcs, making a 225° path, as shown in Figure 3, the calculation grid that was used was 2 mm, the variance of the 2%. Absolute dose measurements for the total VMAT plan, a farmer-type ionization chamber and a solid water phantom were used, as shown in Figure 4. Once the VMAT plan is finalized, all the treatment parameters are exported on the volumetric images of the phantom, where the dose measurement was performed.

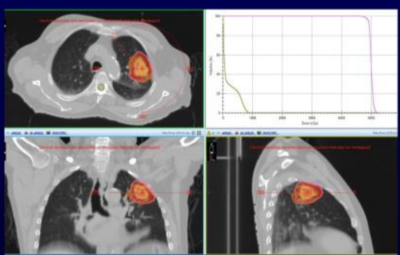

Figure 3. Extracranial stereotaxic treatment planning of a lung Ca

Figure 4. Equipment for absolute dosimetry

A phantom tomography (Octavius 4D) was performed, as shown in Figure 5, and the volumetric images were exported to the SP, the treatment planning was loaded into the phantom and the same calculation parameters were taken into account, obtaining distributions of doses in the phantom, as shown in Figure 6, and finally irradiated in the linear accelerator, in order to compare the distributions of doses measured and calculated by the SP, using the Verisoft software. The acceptance parameters for the gamma analysis were greater than 90% of voxels that have a gamma less than or equal to one, for a dose variation of 3% and a DTA of 3 mm.

Figure 5. Octavius 4D system

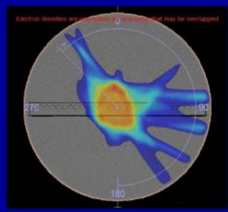

Figure 6. Dose distribution in the phantom

Results

For our study, the percentage difference value between the measured and calculated dose was 2.83%, this indicates an acceptable condition, that is, it guarantees treatment safety, as shown in the following table.

Table 1. Tolerances established in the verification of the calculated and measured absolute dose.a

Assessment	Tolerance	Condition
Measured and calculated dose variation	<3 %	Acceptable
Measured and calculated dose variation	3% – 5%	investigated
Measured and calculated dose variation	>5%	Refused

Figure 7 shows 93% (338,802) of the voxels that meet the gamma criteria analysis (= 3% and = 3 mm), that is, 7% (25,441) of the voxels do not meet the gamma criteria analysis. gamma criterion, or in other words they have γ >1.

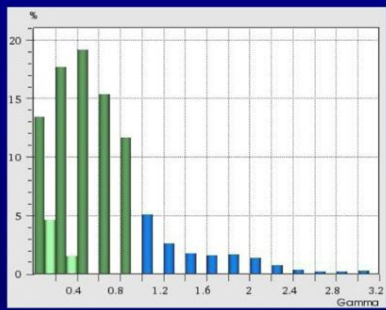

Figure 7. Gamma Histogram

In general, in verifying total dose distributions for IMRT plans, one can distinguish between different high and low dose regions, steep and shallow dose gradient regions, small mismatches or positioning uncertainties can lead to large differences when The calculated and measured dose distributions are compared. Figure 8 shows the comparisons of dose distributions for our study.

The high precision verification system of the linear accelerator was used, this system performs the 4D volumetric acquisition of the patient, using the Cone Beam CT, the displacement corrections were less than 2 mm in the three axes of displacement and 0.5° the angle correction.

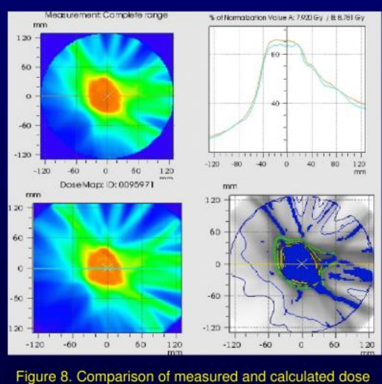

Figure 8. Comparison of measured and calculated dose distribution taking into account the gamma analysis criterion.

conclusions

The method used to carry out quality control in a specific patient at VMAT shows good results, guaranteeing safety in treatments. The verification with the X VI system in 4D, allows the precise location of the target volume, as well as the verification of interfraction. The use of 4D tomographic image acquisition in planning makes it possible to use margins adjusted to the planning volume. Treatment in the IMRT technique in the VMAT modality allows the delivery of the dose in short times.

reference

1. Timmerman R, Paulus R, Galvin J, Michalski J, Straube W, "Stereotactic body radiation therapy for inoperable early stage lung cancer", JAMA, 303, pp. 1070-1076 (2010).
2. Tung S. and Tsao C, "Patient Specific Quality Assurance for IMRT and VMAT", AAPM, 1, pp. 7-14 (2011).
3. Alber M, "Guidelines for the verification of IMRT", ESTRO, 1, pp. 6-32 (2008)

LEIDENFROST EFFECT AND THE HIGH HEAT FLUX COOLING IN TOKAMAKS

Marek Nejman

Faculty of Mechanical Engineering, Czech Technical University in Prague

The Leidenfrost effect is experimentally examined in relation to the boiling crisis and the critical heat flux of tokamak cooling channels. The presence of insulating vapour layer between heated wall and coolant represents a leading limitation of designing the water cooled reactor components [1][2]. The theoretical part of this bachelor thesis provides an overview of nuclear fusion development with focus on major engineering challenges. The practical part consists of series of experimental measurements of the Leidenfrost effect under variable conditions.

Leidenfrost effect and the high heat flux cooling in tokamaks

Marek Nejman, bachelor thesis, 2023

Department of Energy Engineering
Faculty od Mechanical Engineering, CTU in Prague

CTU CZECH TECHNICAL UNIVERSITY IN PRAGUE

Objectives of the thesis

1. Overview of current state of nuclear fusion research and development.
2. Experimental analysis of Leidenfrost effect observed on the dynamic of steel block cooling.
3. Experimental measurements of the Leidenfrost effect on two samples with variable roughness.
4. Comparison of experimental results with measurements of other researchers.
5. Acquiring the Nukiyama boiling curve obtained from the experimental measurements.

Introduction

The Leidenfrost effect is experimentally examined in relation to the boiling crisis and the critical heat flux of tokamak cooling channels. The presence of insulating vapour layer between heated wall and coolant represents a leading limitation of designing the water cooled reactor components [1][2]. The theoretical part of this bachelor thesis provides an overview of nuclear fusion development with focus on major engineering challenges. The practical part consists of series of experimental measurements of the Leidenfrost effect under variable conditions.

Results: cooling of the steel block

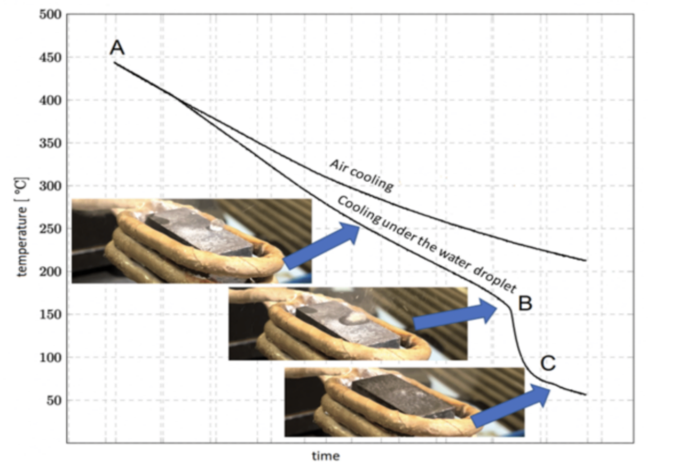

Figure 1: Result of cooling the steel block

Results: experimentally measured Nukiyama curve

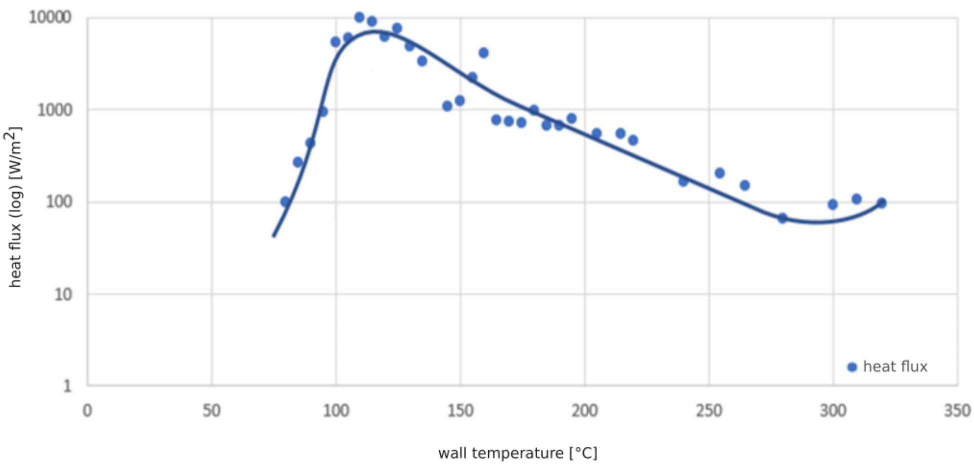

Figure 2: Experimentally measured Nukiyama curve

Results

The Figure 1 shows the results of the first experimental analysis: the dynamic of steel block cooling on air compared to the same sample cooled by periodically impacting water droplets. Top curve represents the characteristics of sample cooled only on air. The lower curve represents cooling under the impacting water droplets. It is divided to 3 parts according to which boiling regime prevails. Schematic setup of the experiment is on the Figure 3.

The Figure 2 shows the second part of experimental analysis: measurements of the droplet evaporation time in relation to the surface temperature. The droplet lifetime measurements were applied to determine the heat flux exhausted in the droplet contact region to build a boiling curve. The Nukiyama curve is based on the average droplet lifetime measurements shown in the Figure 4.

Conclusion

The measurements of droplet lifetime were performed on two samples with variable surface characteristics (roughness). The experimental setup consists of a electrical heater, thermocouple type K, camera and the data acquisition unit. Presented results consist of 4 measurements in each temperature point shown by the green, orange, grey and yellow color and the average value drawn in the blue color. The decreasing droplet lifetime trend at high wall temperatures suggests the increase of exhausted heat flux, an important characteristic of the boiling phenomenon also described by Nukiyama.

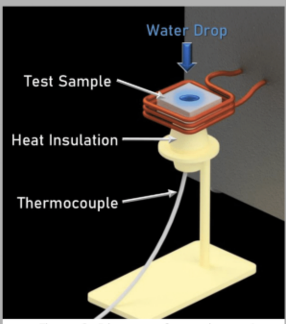

Figure 3: Diagram of experiment 1

Results: measurement of droplet lifetime

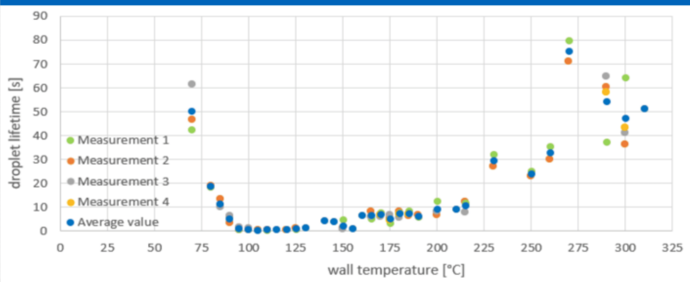

Figure 4: Experimentally measured surface 2

References

[1] Slavomír Entler and Pavel Zácha, High heat flux limits of the fusion reactor water-cooled first wall, Nuclear engineering and technology, doi:10.1016/j.net.2019.03.013
[2] Vojtěch Smolík, Hypervapotron - High Heat Flux Cooling Technology, doi:10.13140/RG.2.2.20940.08328

PERSPECTIVE FUELS FOR NUCLEAR REACTORS

Ondřej Novák

University of west Bohemia

Nuclear fuel is aaspecial chemical compound that is the key to sustain a nuclear chain reaction Radioactive materials that can be fissioned especially uranium and plutonium, are used to make anuclear fuel Currently used fuels are uranium oxide and MOX ("Mixed Oxide") fuels, mainly because of their high melting point and radiradiationstability The problem with these currently used fuels is the low thermal conductivity and the high cost of producing MOX fuels In the future, these fuels could be replaced by pperspectivefuel materialsthat achieve better physical and chemical properties andandreduce nuclear fuel consumptionin nuclear power plants

PERSPECTIVE FUELS FOR NUCLEAR REACTORS

UNIVERSITY OF WEST BOHEMIA

author: **Bc. Ondřej Novák** bachelor thesis supervisor: **Ing. Tomáš Peltan**

Nuclear fuel is a special chemical compound that is the key to sustain a nuclear chain reaction. Radioactive materials that can be fissioned, especially uranium and plutonium, are used to make a nuclear fuel. Currently used fuels are uranium oxide and MOX ("Mixed Oxide") fuels, mainly because of their high melting point and radiation stability. The problem with these currently used fuels is the low thermal conductivity and the high cost of producing MOX fuels. In the future, these fuels could be replaced by perspective fuel materials that achieve better physical and chemical properties and reduce nuclear fuel consumption in nuclear power plants.

METAL FUELS

Metal fuel is composed of **heavy metal**, which is alloyed with **additional metals**. Fuel cells are composed of fuel ingots, a cladding and a gas chamber with gas sealing plugs.

Metal fuels are suitable for **FBR reactors**. [1]

- \+ high density
- \+ thermal conductivity
- \+ low thermal capacity
- \+ longer fuel campaign
- \- swelling
- \- corrosion

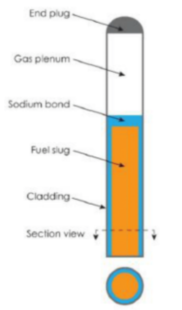

Figure 1. Metal fuel [2]

COMPOSITE NUCLEAR FUELS

The **fuel particles** are dispersed in an inert **non-fuel matrix** made of metal or ceramic material. The fuel particles are arranged to prevent fission gas transport out of the matrix.

Composite fuels are used in reactors, that are used for material testing and radioisotope production. [2] [6]

- \+ fuel-matrix combinations
- \+ high melting temperature
- \- high mass of the reactor
- \- high cost of production
- \- low frequency of measured data

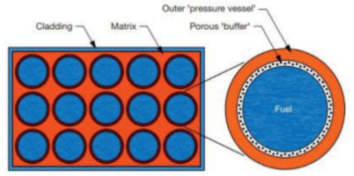

Figure 2. Composite fuel [2]

NITRIDE AND CARBIDE FUELS

Nitride fuels are solutions of **uranium mononitride** (UN) or **plutonium mononitride** (PuN).

These fuels can be used in **Fast Breeder Reactors** (FBR) and **Gas Cooled Fast Reactors** (GFR) from IV Generation of nuclear reactors. [2] [3]

- \+ high density
- \+ thermal conductivity
- \+ high melting temperature
- \+ radiation stability
- \- oxidation
- \- difficult production
- \- spontaneous combustion

LIQUID NUCLEAR FUELS

The basic element is **a fluid** that **carries the fuel**, acts as **a moderator** and **dissipates heat**. Liquid fuels are composed of **a two-liquid mixture** consisting of fission fuel material and fluorides that solidify at low temperatures.

Used in **LFTR** reactors.

- \+ reduces nuclear waste disposal time
- \+ safety (atmospheric pressure)
- \+ high efficiency of power generation
- \- corrosion
- \- development of high temperature materials
- \- uranium separation

TRISO FUELS

This spherical fuel was designed for **High Temperature Gas Cooled Reactors** (HTGR). TRISO fuels are currently only used for **experimental purposes**. The spherical fuel particle is composed of **five independent layers**. [4]

- \+ high efficiency of power generation
- \+ process heat recovery for other industries (petrochemical, manufacture)
- \- high cost of production
- \- complex numerical calculation methods
- \- low frequency of measured data
- \- variable thermal conductivity

Figure 3. TRISO fuel [5]

CALCULATIONS FOR VVER-1000

Table 1. Calculations of multiplication factor depending on enrichment and fuel material

Nuclear fuel	Density	Enrichment	Multiplication factor
Uranium dioxide (UO_2)	10 402,5 kg/m^3	1 %	0,94455 ± 9,4E-05
		2 %	1,23318 ± 9,1E-05
		3 %	1,35355 ± 8,7E-05
		4 %	1,42308 ± 8,8E-05
		5 %	1,46837 ± 8,3E-05
		7,50 %	1,53334 ± 8,1E-05
Metallic uranium (UZr)	17 900,6 kg/m^3	1 %	0,98920 ± 1E-05
		2 %	1,22520 ± 9,7E-05
		3 %	1,33324 ± 9,1E-05
		4 %	1,39554 ± 8,9E-05
		5 %	1,43625 ± 8,7E-05
		7,50 %	1,49513 ± 8,6E-05
Uranium nitride (UN)	13594,5 kg/m^3	1 %	0,86072 ± 1,0E-04
		2 %	1,11325 ± 9,4E-05
		3 %	1,23860 ± 9,3E-05
		4 %	1,31338 ± 9,1E-05
		5 %	1,36348 ± 8,8E-05
		7,50 %	1,43837 ± 8,4E-05
Uranium carbide (UC)	12 606,5 kg/m^3	1 %	1,00838 ± 9,4E-05
		2 %	1,24681 ± 9,1E-05
		3 %	1,35615 ± 9,2E-05
		4 %	1,41848 ± 8,9E-05
		5 %	1,45925 ± 8,9E-05
		7,50 %	1,51802 ± 8,4E-05

All calculations of **the multiplication factor** of individual nuclear fuels for the **VVER-1000** pressurized water reactor were performed using **Serpent Monte Carlo code**. The enrichment of ^{235}U was set from **1 % to 7,5 %**. Population of neutrons was set to **20 000** with **50** inactive cycles and **10 000** active cycles.

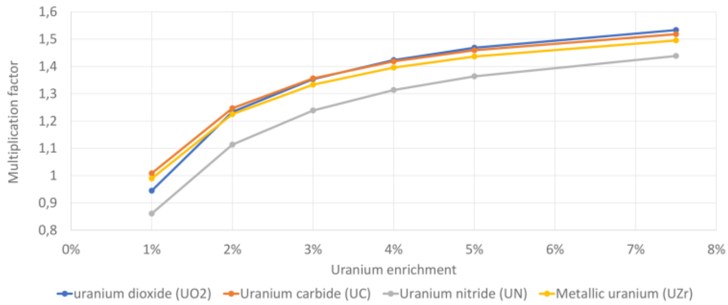

Figure 4. Graph of the multiplication factor

CONCLUSION

From the resulting calculations and the graph of the multiplication factor (*Figure 4*) we can see that the most suitable fuel for the VVER-1000 pressurized water reactor **is uranium dioxide** at an enrichment of **3-5%**, for which the VVER-1000 reactor is designed and constructed. Another potentially suitable fuel could be **UC** or **uranium metal** according to the multiplication factor values. However, for these fuels with higher densities it would be necessary to modify the geometry of the fuel assemblies to achieve higher multiplication factor values, VVER fuel geometry is highly undermoderated for these fuels. On the other hand the overall reactor run time would be longer than for the oxide fuel.

Both **nitride** and **carbide fuels** offer the best option for use in LMFBR reactors in the long term, because of their higher thermal conductivity, higher fission atom density and chemical compatibility with liquid sodium.

REFERENCES

[1] FRWG, Nuclear Metal Fuel: Characteristics, Design, Manufacturing, Testing, Fast Reactor Working Group, 2018.
[2] Comprehensive nuclear materials, Volume 3
[3] R. C. D. H. M. J. M. Ekberg C, Nitride fuel for Gen IV nuclear power systems. J Radioanal Nucl Chem., 2018.
[4] K. Kiegiel, I. H. Koniecko, L. Fuks a G. Kołtuniewicz,Management of Radioactive Waste from HTGR Reactors including Spent TRISO Fuel,"
[5] T. Tracy, „Massachussets Institute of Technology
[6] R. B. H. S. K. B. Robert G. Brrengle, „Aerospace Research Central
[7] R. M. Robert Hargraves, Liquid Nuclear Fuel Reactors, 2011.

MASTER STUDENTS

NUCLEAR POWER AND NON-ELECTRIC APPLICATIONS: DIVERSIFYING EUROPE'S ENERGY LANDSCAPE

Adjoa Amponfi

University of Ghana, Legon

The energy landscape in Europe is continuously evolving, and the dominance of energy sources can change over time due to policy shifts, technological advancements, and changing market conditions. The energy crisis in Europe has been accumulated by a lot of factors and areas; political to environmental.

Nuclear Power and Non-Electric Applications: Diversifying Europe's Energy Landscape

Adjoa Amponfi, *University of Ghana, Legon, aamponfi002@st.ug.edu.gh*

UNIVERSITY OF GHANA

SNAS

Introduction

Mitigating Europe's Energy crisis

The energy landscape in Europe is continuously evolving, and the dominance of energy sources can change over time due to policy shifts, technological advancements, and changing market conditions.

Renewable energy sources in use

The energy crisis in Europe has been accumulated by a lot of factors and areas; political to environmental.

Politics and energy security issues
- Europe has slowly become an area where scenes of re-emerging conflicts and attacks exist.
- For instance, the Russia's invasion of Ukraine, which lead to a cut in Russian gas supply and a surge in energy prices. Natural gas demand in the European Union fell in 2022 by 55 bcm, or 13%, its steepest drop in history.
  - That decline was equivalent to the amount of gas needed to supply over 40 million homes.

Environmental impact on energy crisis
- In Europe, mostly, the usage of fossil fuels has been a primary cause of climate change. Fossil fuels including coal, oil, and natural gas, have been dominant sources of energy for electricity generation, transportation, heating, and industrial processes (like some other parts of the world).
- This has led to a call for reduction in the use of such energy sources and the need for renewable, cleaner and more sustainable energy sources.

Objective

Exploring Non-Electric Applications of Nuclear Energy

This poster is to delve into the realm of non-electric applications of nuclear energy, uncovering its potential to diversify Europe's energy landscape, even beyond electricity generation and supplement current renewables in use.

Nuclear in Energy Diversification

The escalating energy crisis in Europe has brought to light the pressing need for innovative and sustainable solutions to meet the continent's growing energy demands. As the world moves towards a low-carbon future, diversifying energy sources becomes crucial in achieving both energy security and environmental objectives.

- ❑ By reducing dependency on fossil fuels and adopting cleaner energy alternatives, it is possible to mitigate the impacts of climate change and work towards a more sustainable future with secure energy supply.
- ❑ Nuclear energy holds a lot more potential than the conventional use for electricity production that can assist Europe mitigate its energy crisis and consequent effects. But due to low public acceptance which is most likely due to miscommunication or low public knowledge of the stringent safety and regulatory protocols applied in nuclear projects. The figure right below show a graphical overview of the safety to cleaner energy comparison between current energy sources.

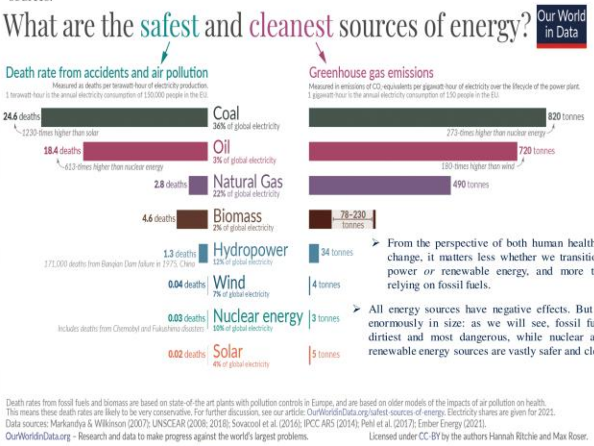

- ➢ From the perspective of both human health and climate change, it matters less whether we transition to nuclear power *or* renewable energy, and more that we stop relying on fossil fuels.
- ➢ All energy sources have negative effects. But they differ enormously in size: as we will see, fossil fuels are the dirtiest and most dangerous, while nuclear and modern renewable energy sources are vastly safer and cleaner.

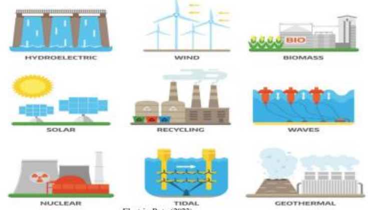

Electric Rate (2023)

- ❑ As Europe faces unprecedented energy challenges, diversifying the energy mix becomes an imperative strategy to enhance energy security and sustainability.
- ❑ While renewable energy sources play a significant role, exploring non-electric applications of nuclear energy can offer a unique set of advantages

Non-Electric Applications of Nuclear Energy

- Non-electric applications of nuclear energy refer to using nuclear energy for purposes other than generating electricity, such as district heating, desalination, hydrogen production, and nuclear-powered ships among others.
- These applications uncover how nuclear power can contribute to a more resilient and diversified energy landscape in Europe.
- In these applications either or both the electrical and thermal energy produced from the reactors are used to power these industrial and large scale processes.
- The explored applications here will include district heating, desalination, and nuclear hydrogen production

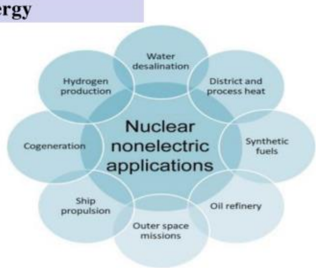

Udalova A. (2020)

District Heating and Cooling

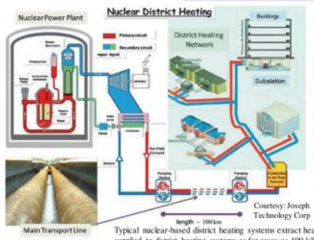

Courtesy: Joseph Technology Corp

Typical nuclear-based district heating systems extract heat from the reactor plant's secondary circuit. Hot water obtained in the process can be supplied to district heating systems as far away as 100 kilometres from the plant. (Power, 2021)

District heating and cooling systems present a compelling opportunity to provide energy-efficient heating and cooling to urban centres.

By integrating nuclear power as a reliable heat source, we can significantly reduce greenhouse gas emissions and reliance on fossil fuels for thermal energy needs

Importance for mitigating Europe's energy crises
- Steady and reliable heat supply, independent of weather fluctuations.
- Substantial reduction in carbon emissions, supporting climate goals.
- Enhanced energy security and resilience against fuel price volatility.

Nuclear Desalination

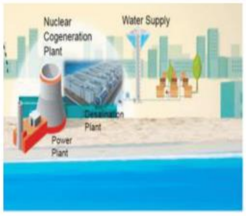

Schmidt et al (2021)

Quality water scarcity poses a significant challenge in various regions of Europe.

Nuclear desalination emerges as a sustainable and energy-efficient solution to meet the growing demand for fresh water while minimizing environmental impacts.

Importance for mitigating Europe's energy crises effect on water
- Consistent and abundant freshwater supply from seawater.
- Reduced dependence on traditional water sources, mitigating water stress.
- Synergistic utilization of nuclear energy for both electricity and water production.

Nuclear Hydrogen

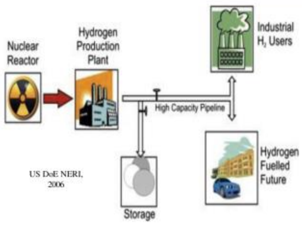

US DoE NERI, 2006

Hydrogen holds immense potential as a clean and versatile energy carrier.

Nuclear hydrogen production, facilitated by nuclear reactors, presents an opportunity to drive a more efficient way of hydrogen production and the transition to a low-carbon economy in Europe

Importance for mitigating Europe's energy crises effect on water
- Carbon-free hydrogen production, contributing to emission reduction.
- Meeting industrial needs and decarbonizing manufacturing processes.
- Fuelling hydrogen-based transportation for a sustainable mobility future.

Advantages and Disadvantages of Nuclear Energy Non-Electric Applications

Advantages:
- Low carbon emissions, supporting climate objectives.
- Enhanced energy security and reduced import dependency.
- Diverse applications for versatile utilization

Disadvantages:
- Safety considerations and public perception
- Regulatory framework for non-electric applications.
- Cost and investment considerations.

Innovations and Research

Ongoing Innovations:
- Advanced reactor designs for versatile heat and hydrogen production.
- Technological advancements in desalination efficiency and safety.
- Collaborative projects fostering interdisciplinary research.

The Road Ahead:
- Supporting pilot projects and real-world implementations.
- Policy backing for nuclear energy diversification research

Conclusion

- Nuclear energy holds immense potential beyond electricity generation.
- By exploring non-electric applications such as district heating, desalination, and nuclear hydrogen production; a diverse, resilient, and sustainable energy landscape can be created for Europe
- Non-electric nuclear applications complement Europe's transition to a low-carbon future.
- District heating, desalination, and nuclear hydrogen have a transformative impact on multiple sectors.
- Thoughtful policy and research investments are key to unlocking the full potential of nuclear energy diversification

Bibliography

1. Elder R., Allen R., (2008). Nuclear heat for hydrogen production: Coupling a very high/high temperature reactor to a hydrogen production plant. *Progress in Nuclear Energy. 51(3), 500-525*
2. EU External Action, (2021). EU Security, Defence and Crisis response. Retrieved on: 30th July, 2023. Available at : https://www.eeas.europa.eu/eeas/eu-security-defence-and-crisis-response.
3. Electric Rate, (2023). Importance of Green Energy Sources. Available at: https://www.electricrate.com/green-energy/clean-energy-benefits/. Retrieved on: 20th July, 2023.
4. Udalova A. (2020). 10 - Nonpower applications of nuclear technology. *Nuclear Reactor Technology Development and Utilization. Pg: 319-341. https://doi.org/10.1016/B978-0-12-818483-7.00010-X*
5. Power (2021). District Heating Supply from Nuclear Power Plants. Retrieved on: 10th July 2023. Retrieved from: https://www.powermag.com/district-heating-supply-from-nuclear-power-plants/
6. Zeniewski P., Molnar G., Hugues P., (2023). Europe's energy crisis: What factors drove the record fall in natural gas demand in 2022?. *International Energy Agency. Commentary.*
7. Effect of wide observation of nature in renewable energy engineering education - Scientific Figure on ResearchGate. [accessed 30 July, 2023]. Available from: https://www.researchgate.net/figure/Wide-observation-to-renewable-energy-sources_fig1_355433390
8. Schmidt M. J., Gude G. V., (2021). Nuclear cogenera2(100044)tion for cleaner desalination and power generation – A feasibility study. *Cleaner Engineering and Technology.*

CORROSION OF STRUCTURAL MATERIALS IN MOLTEN SALT ENVIROMENTS

Anna Golubko, Jana Rejková, Marie Kudrnová

University of Chemistry and Technology, Department of Power Engineering, Prague, Czech Republic

Molten saltaltmixtures, such as chlorides, nitrates, nitrites and carbonates, are well knowknownfor theirtheirhigh heat capacities and low melting points SaidSaidsaltsare mostmostly usedin CSP (Concentrated Solar Power) and TES (Thermal Energy Storage) systems but also in MSR (Molten Salt Reactors The aforementioned technologies are heavily researched, or already utilized in the global energy field The requirements for the construction materials are however high, and not all alloys can withstand such conditionsconditions. ThisThisposterprovides information about the research findings reported in thethediploma thesis of the same name

Corrosion of structural materials in molten salt environments

Anna Golubko, Jana Rejková, Marie Kudrnová
anne.golubko@gmail.com
University of Chemistry and Technology, Department of Power Engineering, Technická 5, Prague 6, 16628, Czech Republic

Molten salt mixtures, such as chlorides, nitrates, nitrites and carbonates, are well known for their high heat capacities and low melting points. Said salts are mostly used in CSP (Concentrated Solar Power) and TES (Thermal Energy Storage) systems but also in MSR (Molten Salt Reactors The aforementioned technologies are heavily researched, or already utilized in the global energy field. The requirements for the construction materials are however high, and not all alloys can withstand such conditions. This poster provides information about the research findings reported in the diploma thesis of the same name.

Experiments and results

Five tested materials that were chosen for aforementioned experiments were samples of nickel alloys such as Inconel 601, 617 and 625, Hastelloy C-22, and the experimental material MoNiCr. For the purposes of the diploma thesis that this presentation is based on, five chosen materials were tested during two experiments that were carried out in molten eutectic salt LiCl-KCl (58,2-41,2 wt.%) under an inert argon atmosphere, each with a different temperature setting, and two comparative experiments under an inert argon atmosphere without the salt mixture, also with different temperature settings. All materials were then analysed using X-Ray Photoelectron Spectrometry (XPS) and Scanning Electron Microscopy (SEM). All data obtained from analysis was carefully compared in order to determine which of the tested materials show the highest corrosion resistance.

The spectra obtained from XPS analysis were summed up in tables. They showed a certain trend on the surface of all tested materials, which confirms that chromium and nickel compounds were formed during experiments. High oxygen content on the surface of all tested materials suggests that oxides were present. Based on the research done for the thesis, the formation of chromium oxides under similar experimental conditions is highly possible.

Inconel 601, 617, 625, Hastelloy C-22 and to some degree even MoNiCr showed that most chromium oxides formed during Experiments 2 and 4, which were carried out without a salt mixture. Carbon found on the surface of all of the materials is most likely contamination absorbed by the materials from the atmosphere in the laboratory. The sample of Inconel 625 (Figure 1.) showed greatest corrosion damage after Experiment 1. The Surface of said material (Figure 2.) showed signs of exfoliation and developed a thick corrosion product layer of 0,6–0,8 μm. The highest corrosion rate was observed during Experiment 2. The surface of Inconel 601 (Figure 3.) showed signs of pitting and cavities reaching almost 2,5 μm under the surface. A corrosion product layer formed on the surface had a maximum thickness of 0,2 μm.

Table 1.: Conditions of the experiments.

	Temperature [°C]	Pressure [MPa]	Environment	Duration [h]
Experiment 1	440	0,2	Argon, LiCl-KCl	500
Experiment 2	600	0,2	Argon	500
Experiment 3	500	0,2	Argon, LiCl-KCl	500
Experiment 4	400	0,2	Argon	500

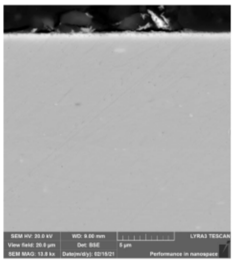

Figure 1.: Photo of a cross section of the sample Inconel 625 after Experiment 1.

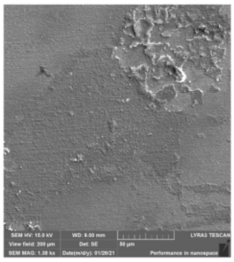

Figure 2.: Photo of a surface of the sample Inconel 625 after Experiment 1.

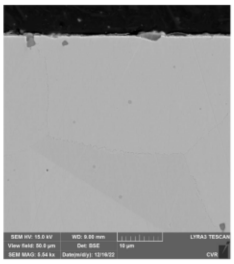

Figure 3.: Photo of a cross section of the sample Inconel 601 after Experiment 2.

The Sample of Inconel 625 (Figure 4) showed signs of exfoliation and corrosion product layer separation with the top layer thickness being 0,2 μm. Hastelloy C-22 (Figure 5) showed signs of pitting corrosion and possible exfoliation of the thin product layer of 0,3 μm. Inconel 617 (Figure 6) showed pitting corrosion and some crack propagations after Experiment 3. The corrosion product layer formed on the surface of Inconel 617 was only 0,3 μm thick.

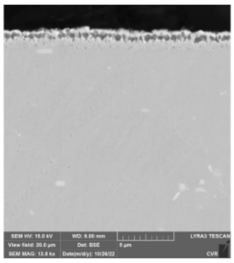

Figure 4.: Photo of a cross section of the sample Inconel 625 after Experiment 3.

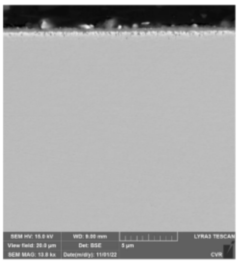

Figure 5.: Photo of a cross section of the sample Hastelloy C-22 after Experiment 3.

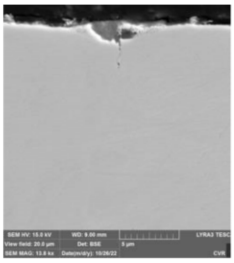

Figure 6.: Photos of a cross section of the sample Inconel 617 after Experiment 3.

The sample of MoNiCr, which was quite resistant during previous experiments, showed the highest levels of corrosion after Experiment 4. The Layer of products that formed on the surface had a maximum thickness of 0,6 μm. The photos below capture pits (Figure 7) and a heavily affected surface (Figure 8).

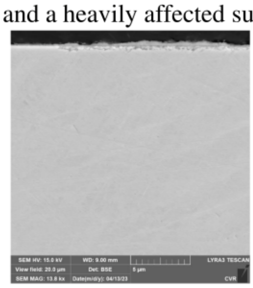

Figure 7.: Photo of a cross section of the sample MoNiCr after Experiment 4.

Figure 8.: Photo of a surface of the sample MoNiCr after Experiment 4.

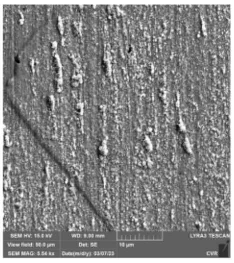

Conclusion

All tested samples showed some degree of resistance, although none of them resisted all of the conditions and environments. Different conditions require different construction materials, and the presented research fully proves that. Based on all of the results, it could be claimed that Inconel 617 and MoNiCr performed best across all of the experiments. It could be assumed that such results were due to low iron content in both materials in their pre-experiment states, as well as each containing high levels of molybdenum (MoNiCr) and cobalt (Inconel 617).It is safe to say that more research and experimentation must be done before any of the materials can be used long-term in high temperature and/or molten salt environments.

This research work has been carried out within the ADAR project (Accelerator Driven Advanced Reactor). Authors gratefully acknowledge financial support from the Ministry of Education, Youth and Sports of the Czech Republic under INTER-ACTION research program (project No. LTAUSA18198).

STUDY ON NEUTRONIC AND THERMOHYDRAULIC OF LEAD COOLED REACTOR WITH URANIUM NITRIDE FUEL

Ondřej Lachout

Czech Technical University, Faculty of Nuclear Sciences and Physical Engineering, Department of Nuclear Reactors, Czech republic.

The objective of the project aims to design a passively safe lead-cooled Gen-IV reactor with $(U_{0.95-x}Pu_xAm_{0.05})N$ fuel. The initial phase of the study involves fuel geometry determination for the cladding to survive a transient temperature of 1000 K for 200 s using an analytical approach. Subsequently, fuel composition is adjusted by Pu concentration to reach minimum reactivity swing for BU_{FIMA}= 6 % using a neutronic code Serpent2. Critical mass and number of fuel rods were determined for the system to by critical. Consequently, conversion ratio, minor actinide burning rate, and reactivity coefficients, such as Doppler constant, temperature reactivity coefficients, axial and radial reactivity coefficients were calculated. Furthermore, UTOP and ULOF transients were simulated and analysed using BELLA software. The whole calculation process was iterative to obtain the most relevant results.

Study on Neutronic and Thermohydraulic of Lead Cooled Reactor with Uranium Nitride Fuel

Author: Ondřej Lachout [1,2]
Co-author: Jakub Mátl [1,2]
[1] Czech Technical University, Faculty of Nuclear Sciences and Physical Engineering, Department of Nuclear Reactors, Czech republic
[2] KTH Royal Institute of Technology, Department of Physics, Nuclear Engineering, Sweden

ABSTRACT:
The objective of the project aims to design a passively safe lead-cooled Gen-IV reactor with $(U_{0.95-x}Pu_xAm_{0.05})N$ fuel. The initial phase of the study involves fuel geometry determination for the cladding to survive a transient temperature of 1000 K for 200 s using an analytical approach. Subsequently, fuel composition is adjusted by Pu concentration to reach minimum reactivity swing for BU_{FIMA}= 6 % using a neutronic code Serpent2. Critical mass and number of fuel rods were determined for the system to by critical. Consequently, conversion ratio, minor actinide burning rate, and reactivity coefficients, such as Doppler constant, temperature reactivity coefficients, axial and radial reactivity coefficients were calculated. Furthermore, UTOP and ULOF transients were simulated and analysed using BELLA software. The whole calculation process was iterative to obtain the most relevant results.

FUEL GEOMETRY DETERMINATION

Determination of fuel geometry refers to a fuel pin radius and fuel pin pitch calculations using an analytical approach. The methodology is based on the demand for a cladding tube (15-15Ti) to survive a transient temperature of 1000 K for 200 s.
The process is based on solving a series of analytically derived equations presented in [1]. In the following text the process will be simplistically described:

- Larson-Miller parametr *(LPM)* is calculated for cladding to withstand the transient,
- hoop stress *(σ_{hoop})* and pressure of fission gas *(P_{fg})* are determined based on 15-15Ti cladding tube experimental data,
- height of gas plenum *(H_{plenum})* is optimized to accommodate full fission gasses release (for Nobel gasses fission yields see Tab. 1),
- in case for natural convection to be sufficient to evacuate residual heat from the core during ULOF transient, natural velocity of coolant *(v_{nat})* is determined satisfying the condition for the coolant flow to remain turbulent,
- nominal pressure drop *(ΔP_{nom})*, hydraulic diameter *(D_h)*, coolant flow area *(A_{flow})*, diameter of fuel pin *(D_{rod})* and gap between fuel pins *(D_{wire})* were calculated satisfying cladding resistance during the transient.

All calculated parameters are presented in Tab. 2 and fuel geometry is visualised in Fig. 1.

Tab. 1 - *Nobel gasses yield per fission.*

Y_{Xe} (%)	Y_{Kr} (%)	Y_{He} (%)	Y_{FG}^{tot} (%)
22.83	1.76	16.24	40.82

Tab. 2 - *Summary of calculated parameters.*

Parameter	Value	Parameter	Value
σ_{hoop} (MPa)	367.87	ΔP_{nom} (kPa)	128.75
P_{fg} (MPa)	36.78	D_H (cm)	0.462
H_{plenum} (cm)	64.0	A_{flow} (cm^2)	0.231
H_{ch} (cm)	164.0	D_{rod} (cm)	1.078
v_{nat} (m/s)	0.144	D_{wire} (cm)	0.196
v_{nom} (m/s)	1.44	P (cm)	1.274
P/D (-)	1.18	r_{fuel} (mm)	4.72
δ_{clad} (mm)	0.472	δ_{gap} (mm)	0.2

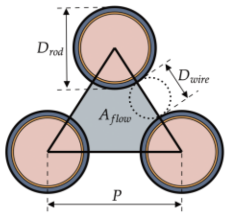

Fig. 1 - *Fuel channel visualization.*

NEUTRONIC CALCULATIONS

Neutronic calculations were performed in neutronic code Serpent2. A neutronic model was itteratively modified to above calculated fuel geometries, coolant and fuel properties.

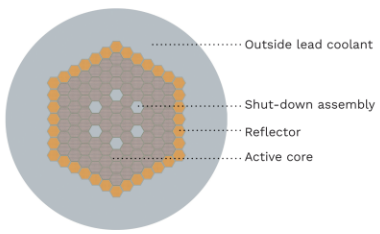

Fig. 2 - *Active core design description.*

Tab. 3 - *Core design parameters.*

Parameter (Units)	Value
Fuel density - ρ_{fuel} (g/cm^3)	13.32
Lead density - ρ_{Pb} (g/cm^3)	10.471
Fuel assemblies - N_{FA} (-)	85
Fuel pins per assembly - N_{FP} (-)	169
Fuel lattice pitch (cm)	17.4
Reactivity control assemblies (-)	6
Reflector assemblies (-)	36
Reactor thermal power - P_{th} (MWt)	96
Critical fuel mass - m_{fuel} (t)	13.32
Coolant total mass - m_{Pb} (t)	363

a) Fuel optimization

Among others, one of the promising advantages of Gen-IV reactors is the possibility to burn minor actinides (MA). By mixing MA with fuel, the spent fuel radiotoxicity can be significantly reduced. More specifically, the time that the spent fuel repository requires of function may be lowered by two orders of magnitudes. Another great aspect is that the overall volume of the spent fuel repositories can be reduced by a factor of six. [1]
Adding MA has a negative impact on reactor behaviour, mainly on reactivity coefficients and passive safety. This is a great challenge to deal with.
The major radio-toxic contributor in a spent nuclear fuel is Am. From the reasoning above two americium isotopes were added to fuel in 5% concentration, which corresponds to generally known assumptions.
Gen-IV fuels are assumed to use fuels based on a combination of Uranium and Plutonium. For Uranium, so-called Depleted uranium (DU), which is a remnant after fuel enrichment, is used.
For Plutonium, the so-called Reactor Grade Plutonium (RGPu), is used. Two isotopes of Am were used in ratio ^{241}Am/^{243}Am = 60/40. In this report, nitride fuel, with 0.941 % ^{15}N concentration, is investigated.
Taking into consideration aforementioned, fuel to be optimized is $(U_{0.95-x}Pu_xAm_{0.05})N$, where x is searched plutonium concentration, for which the fuel composition yields a minimum reactivity swing at BU_{FIMA} = 6 %. This way the criticality of the reactor during fuel burnup is affected the least.

Optimal Plutonium concentration was determined to be 12.2 % resulting in optimized fuel to be $(U_{0.828}Pu_{0.122}Am_{0.05})N$. Curves of reactivity depending on BU_{FIMA} for different Plutonium concentrations are presented in Fig. 3. In Fig. 4 detailed shot of the reactivity swing for sought optimal fuel fitted by a parabolic curve is presented. During depletion the maximum reactivity swing for this configuration was determined to be *$\Delta\rho$=(-985±64)* pcm. The curve, that was derived is a parabola. The shape of the reactivity over burn-up depends mainly on linear power, which for studied reactor design is 6.676 kW/m. For the trend to be opposite (concave parabola) power density would have to be (at least 2.5 times) increased.

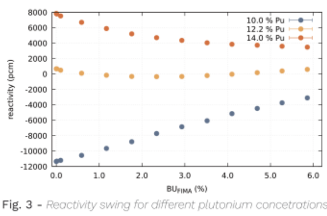

Fig. 3 - *Reactivity swing for different plutonium concetrations.*

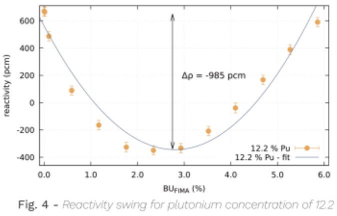

Fig. 4 - *Reactivity swing for plutonium concentration of 12.2 %.*

b) Minor actinides burning rate

Optimized fuel composition includes 5 % of two americium isotopes. This isotopes were extracted from already burned fuel to reduce its radio-toxicity and added to the fuel composition. The burning rate of MA is an interesting parameter to be examined, because it tells us how much of initial americium mass will be „burned". From initial mass 642 kg of Am, more than 170 kg of it was „burned" over 21 years in reactor. For streamlining burning of MA one can see, that this process needs to be repeated several times. The burning rate can be determined as:

$$\mathrm{MA_{BR}} = \frac{dm(Am)}{dE_{\mathrm{rel}}} = 9.20\ \mathrm{kg/TWh}.$$

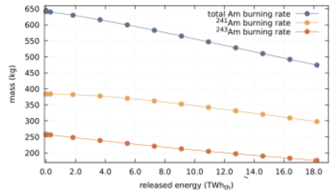

Fig. 5 - *Minor actinides burning rate.*

c) Fuel breeding

Fuel breeding is an important feature for future Gen-IV reactors. As was discussed before, the fast neutron spectrum of the reactor contributes to better neutron economy and higher possible burnup. It is desired to have a conversion ratio higher than unity (one of the Gen-IV reactor definition). Relation for in-pile conversion ratio *(CR_{ip})* is given by equation (1), derived by Wallenius. The needed parameters were calculated using Serpent2 at BoL.

$$CR_{\mathrm{ip}} = \frac{\sum_{\mathrm{A},m} \sigma_{\mathrm{c}}\left({}^{m}A\right) C\left({}^{m}A\right) \eta\left({}^{m+1}A\right)}{\sum_{\mathrm{A},m} \sigma_{\mathrm{f}}\left({}^{m}A\right) C\left({}^{m}A\right) \eta\left({}^{m}A\right)} = 1.78. \tag{1}$$

d) Safety parameters

Safety parameters are essential for Gen-IV reactor design. Safety parameters are natural parameters, which determine reactor behaviour in normal operation, abnormal and emergency conditions. They determine how the change in power and temperature may affect the reactivity considering different phenomena.
For the presented reactor design safety parameters were calculated at BoL and are presented in Tab. 4.

Tab. 4 - *Safety parameters calculated at BoL.*

Parameter (Units)	Value
β_{eff} (pcm)	389
Λ_{eff} (μs)	0.717
K_D (pcm)	-338 ± 57
α_{Pb}(core) (pcm/K)	0.171 ± 0.031
α_{Pb}(out) (pcm/K)	-0.158 ± 0.038
α_{axial} (pcm/K)	-0.247 ± 0.037
α_{radial} (pcm/K)	-0.864 ± 0.018

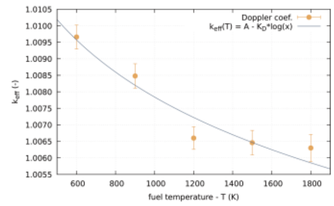

Fig. 6 - *Doppler reactivity coefficient.*

THERMOHYDRAULIC ANALYSIS

Thermohydraulic analysis was performed using BELLA software developed at KTH. The code is based on point kinetics and balance equations for mass, energy and momentum, which are generally applied to the core and primary system components.

a) UTOP

Unprotected Transient Overpower (UTOP) is initiated when a control rod is unintentionally withdrawal from the core, the control system does not induce reactor scram and the pumps maintain the nominal coolant flow through the core. The transient was analysed for reactivity insertion of 0.5 $ at BoL. Temperatures of fuel, cladding and coolant during the transient are visualized in Fig. 7.
Temperatures are immediately increased and peaked after a tenths of seconds after the beginning of the transient. After that, due to overall negative reactivity coefficients, the temperature decreases and finds a new equilibrium state.

b) ULOF

Unprotected Loss of Flow (ULOF) transient is initiated when the power of the primary pump is lost, or blockage of a coolant channel occurs. Due to the lack of SCRAM, the only mechanism for decreasing the reactor power are reactivity feedbacks. If the sum of all reactivity feedbacks is negative, the core becomes sub-critical, power is reduced, and the fuel temperature decreases, see Fig. 8.

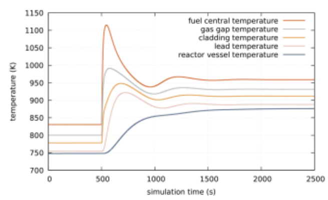

Fig. 7 - *Simulation of UTOP transient.*

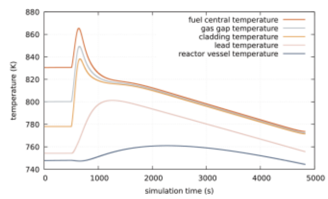

Fig. 8 - *Simulation of ULOF transient.*

CONCLUSION

Fuel geometry was determined satisfying the condition to survive a transient temperature of 1000 K for 200 s. Fuel composition $(U_{0.828}Pu_{0.122}Am_{0.05})N$ was found yielding the minimum reactivity swing at BU_{FIMA}= 6 %. Maximal reactivity swing during fuel burnup was found to be $\Delta\rho$=(-985±64) pcm. Critical mass of (m_{fuel} = 13.32 t) and number of fuel rods (N_{rod} = 14365) were determined for the system to by critical. Consequently, conversion ratio equal to CR_{ip} = 1.78, minor actinides burning rate 9.20 kg/TWh, and reactivity coefficients, such as Doppler constant, temperature reactivity coefficients, axial and radial reactivity coefficients were calculated. Furthermore, UTOP and ULOF transients were simulated and analysed using BELLA software. The maximum temperatures during both transients remains below safety limits. The whole calculation process of neutronic and thermohydraulic calculations was iterative to obtain the most relevant results.

ACKNOWLEDGEMENT:

The study was presented as a final project for subject Generation IV Reactors taught by Janne Wallenius at KTH in 2023. Most of the presented equations and calculation procedures are inspired by the lectures or taken from a textbook [1], alternatively articles [2], [3].

REFERENCES

[1] J. Wallenius and S. Bortot, "Fast neutron generation IV reactors," 2023 [Unpublished book]

[2] F. Dehlin, J. Wallenius, and S. Bortot, "An analytic approach to the design of passively safe lead-cooled reactors," Annals of Nuclear Energy, vol. 169, p. 108971, 2022. [Online]. Available: https://www.sciencedirect.com/science/article/pii/S0306454922000068

[3] J. Wallenius, S. Qvist, I. Mickus, S. Bortot, P. Szakalos, and J. Ejenstam, "Design of sealer, a very small lead-cooled reactor for commercial power production in off-grid applications," Nuclear Engineering and Design, vol. 338, pp. 23–33, 2018. [Online]. Available: https://www.sciencedirect.com/science/article/pii/S0029549318301821

NEUTRONIC ANALYSIS OF A HEAT-PIPE COOLED REACTOR

Josef Sabol, Jan Frýbort

Faculty of Nuclear Sciences and Physical Engineering , Department of Nuclear reactors, Czech Technical University in Prague

Heat-pipe cooled reactors belong to the group of nuclear reactors using heat pipes filled with liquid metals (such as sodium or potassium) to cool the core. They are composed of a reactor core, heat pipes, reflector, regulation system, shielding, and electrical conversion system. Due to the passive heat removal system, there is no need to use closed cooling loops with pumps inside the reactor core, and the reactor can be operated with reduced requirements for external systems. Consequently, this system can be used in remote locations without access to an electrical grid (such as research and military stations), or it can be used for space applications (Moon bases or spacecrafts)

NEUTRONIC ANALYSIS OF A HEAT-PIPE COOLED REACTOR

JOSEF SABOL*, JAN FRÝBORT
**corresponding author: saboljos@cvut.cz*

Faculty of Nuclear Sciences and Physical Engineering
Department of Nuclear Reactors
Czech Technical University in Prague

INTRODUCTION

Heat-pipe cooled reactors belong to the group of nuclear reactors using heat pipes filled with liquid metals (such as sodium or potassium) to cool the core. They are composed of a reactor core, heat pipes, reflector, regulation system, shielding, and electrical conversion system. Due to the passive heat removal system, there is no need to use closed cooling loops with pumps inside the reactor core, and the reactor can be operated with reduced requirements for external systems. Consequently, this system can be used in remote locations without access to an electrical grid (such as research and military stations), or it can be used for space applications (Moon bases or spacecrafts).

This poster further deals with a detailed neutronic study of the SPR Design-B reactor concept from Idaho National Laboratory, which was developed in 2017 [1].

1. REACTOR DESIGN

The thermal power output of the reactor is 5 MW. For safety reasons, the reactor core is divided into 6 segments separated by double stainless steel wall, each segment contains 352 fuel rods (19.75% enrichment in form of UO_2) and 204 heat pipes (filled with liquid potassium). The stainless steel cladding is filled with helium.

Each of the segments is filled with liquid sodium, which works as a heat transfer medium between fuel and heat pipes. Above and below the reactor core is a stainless steel axial reflector. The radial reflector consists of Al_2O_3, a helium gap, stainless steel shielding to protect from gamma radiation and enriched B_4C to protect it from neutron irradiation.

For reactivity control, 12 rotating control drums situated around the reactor core with semicircular cut-outs of enriched B_4C are used. The rotation of the drums can be used to increase/decrease neutron absorption and thus control the reactivity. Safety rods (inner and annular outer) that are used for safe shutdown are also made up of enriched B_4C.

The outer diameter of the reactor is 2 m and the height is also 2 m. The vertical and horizontal cross sections of the model are shown in Figure 1.

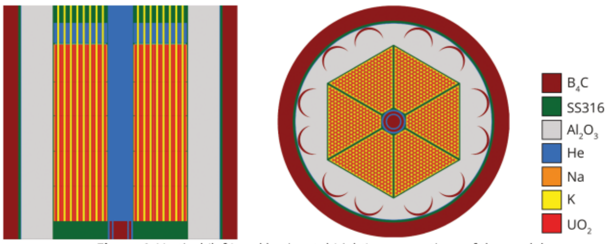

Figure 1: Vertical (left) and horizontal (right) cross sections of the model.

2. RESULTS

Calculations with neutron transports and the depletion calculations were performed using stochastic Monte-Carlo code Serpent 2 in version 2.1.32 [2] and with nuclear data library ENDF/B-VIII.0 [3].

2.1 REACTIVITY CALCULATIONS

Reactivity can be controlled in several ways. The most important is control by control drums rotation, which are changing neutron absorption. Shutdown rods are used for safety shutdown. The maximum excess reactivity at the Beginning of Life (BOL) is:

$$\rho_{\max}^{\mathrm{BOL}} = (1543 \pm 2)\ \mathrm{pcm}.$$

The dependency of k_{eff} on control drums rotation angle is shown in Animation 1-a (rods inside) and 1-b (rods outside). The dependency of k_{eff} on shutdown rods position is shown in Animation 1-c.

a) b) c) d)

Animation 1: a) dependency of k_{eff} on control drums rotation angle with rods inside, b) with rods outside, c) dependency of k_{eff} on shutdown rods position in critical configuration, d) dependency of power distribution on control drums rotation angle.

To achieve criticality, it is necessary to rotate the control drums by 51° and 318°, respectively. For a more even power distribution, the 51° position is preferable (as can be seen in Figure 2, or in Animation 1-d), therefore all the following calculations were done for this position.

Table 1 shows the worths of the safety components and compares them with the values from [1]. The calculations in this work showed lower k_{eff}, which is associated with lower BOL excess reactivity. When comparing the worths of the safety systems, the results in this work are slightly higher.

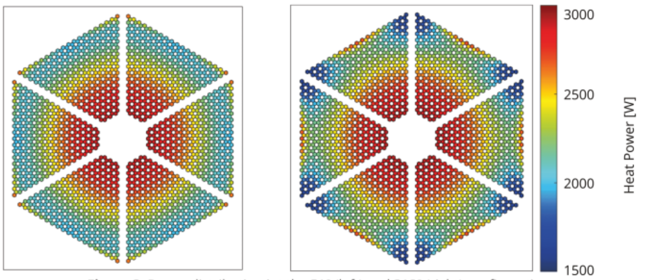

Figure 2: Power distribution int the 51° (left) and 318° (right) configuration.

Table 1: Worths of the safety components.

	MCNP 6.1 [1]	**SERPENT 2**
	ENDF/B VII.0	ENDF/B VIII.0
Critical Drums Rotation [°]	56	51/318
β_{eff} [%]	0.7	0.7199 ± 0.0002
BOL Excess Reactivity [pcm]	2 359	$1\,543 \pm 2$
Total Drums Worth [pcm]	9 079	$10\,677 \pm 3$
Individual Drum Worth [pcm]	770	866 ± 3
Inner Rod Worth [pcm]	6 013	$6\,148 \pm 3$
Annular Rod Worth [pcm]	7 504	$7\,754 \pm 3$
Both Rods Worth [pcm]	-	$8\,583 \pm 3$

2.1 REACTIVITY COEFFICIENTS

The fuel Doppler broadening effect has the greatest influence on the change in reactivity with temperature change. Other thermal aspects include axial elongation of fuel rods, radial expansion of reflector, volume expansion of sodium, and radial expansion of fuel grids. Table 2 shows the calculated temperature reactivity coefficients in these cases.

All the temperature reactivity coefficients are negative. Most of all obtained values are smaller in absolute value compared to those in [1]. In addition, the influence of the expansion of fuel grids and thus the changing fuel pitch was also calculated. This aspect was not considered in [1], however, its value is not negligible, and it is the second largest reactivity coefficient after the fuel Doppler broadening.

Table 2: Temperature reactivity coefficients.

	MCNP 6.1 [1]	**SERPENT 2**
	ENDF/B VII.0	ENDF/B VIII.0
Fuel Doppler Broadening [pcm/K]	-0.9485	-0.608 ± 0.010
Fuel Axial Elongation [pcm/K]	-0.3234	-0.242 ± 0.005
Radial Reflector Expansion [pcm/K]	-0.1575	-0.142 ± 0.004
Sodium Volume Expansion [pcm/K]	-0.0723	-0.16 ± 0.03
Grids Expansion [pcm/K]	-	-0.586 ± 0.013
Total [pcm/K]	**-1.5017**	**1.74 ± 0.03**

2.3 DEPLETION CALCULATION

The multiplication factor decreases roughly linearly during the depletion. Due to the small burnup (1.77 MWd/kgU over 5 years at nominal power), the reactor is still supercritical at the End of Life (EOL):

$$\rho_{\max}^{\mathrm{EOL}} = (1297 \pm 9)\ \mathrm{pcm}.$$

The effect of burnup can also change the worths of control elements because it shifts the power distribution to the periphery, leading to greater neutron leakage. Since the reactor is regulated by control drums, their efficiency should change.

There was an increase in all worths during the calculation, but due to the larger statistical uncertainties, the worths of the elements are roughly constant over time. Thus, during operation, it would be possible to maintain criticality using only a slight rotation of the control drums.

The effect of burnup should also shift the power distribution to the periphery. In this analysis, the neutron flux was not sufficient and even in 5 years there was no significant shift. A maximum difference was achieved up to 1% between BOL and EOL, but this difference may be due to statistical uncertainties. The power distribution is roughly constant over time. Thanks to low burnup, xenon dead time also does not occur.

CONCLUSION

In this poster, the neutronic model of the SPR Design-B nuclear reactor concept is described and basic safety analyses are calculated. The results obtained by Serpent 2 code and ENDF/B-VIII.0 nuclear data library are discussed and also compared with the original study [1], where MCNP 6.1 code with ENDF/B-VII.0 nuclear data library was used for the calculations.

All the values obtained are very similar. All feedback coefficients are negative, as well as the worths of safety elements are high enough to shutdown the reactor. The worths increase during depletion, but due to the larger statistical uncertainties, they are roughly constant over time. Thanks to low burnup, xenon dead time also does not occur.

The biggest differences are in the lower k_{eff} in this work. This may be due to a different model, a different nuclear data library with different code, or due to an axial neutron leakage (there was not described exact position and shape of radial reflectors).

REFERENCES

[1] J. W. Sterbentz, J. E. Werner, A. J. Hummel, et al. Preliminary Assessment of Two Alternative Core Design Concepts for the Special Purpose Reactor 2017. https://doi.org/10.2172/1413987
[2] J. Leppänen, M. Pusa, T. V. et al. The Serpent Monte Carlo code. In *Annals of Nuclear Energy*, vol. 82, pp. 142–150. 2015. https://doi.org/10.1016/j.anucene.2014.08.024
[3] D. A. Brown, M. B. C. et al. ENDF/B-VIII.0: The 8th major release of the nuclear reaction data library with CIELO-project cross sections, new standards and thermal scattering data. In *Nuclear Data Sheets*, vol. 148, pp. 1–142. 2018. Special Issue on Nuclear Reaction Data. https://doi.org/https: //doi.org/10.1016/j.nds.2018.02.001

FACULTY OF NUCLEAR SCIENCES AND PHYSICAL ENGINEERING CTU IN PRAGUE

3D TRANSIENT CFD SIMULATION OF AN IN-VESSEL LOSS-OF-COOLANT ACCIDENT IN THE EU DEMO WCLL BREEDING BLANKET

Mauro Sprò

NEMO group, Dipartimento Energia , Politecnico di Torino, Torino, Italy

- An unprotected plasma transient event could cause the break of a portion of the BB, leading to an in vessel LOCA transient
- The pressurized coolant will be released inside the vacuum chamber, giving rise to a flashing jet
- VV failure criterion is local (i.e. pressure peak on gyrotron diamond windows) need for local analyses in support to global modelling

Politecnico di Torino
Department of Energy "G.Ferraris"

3D Transient CFD Simulation of an In-Vessel Loss-of-Coolant Accident in the EU DEMO WCLL Breeding Blanket

Download the paper!
M. Sprò et al., Energies 16(9):3637, 2023
10.3390/en16093637

Candidate: Mauro Sprò
Supervisors: Dr. Antonio Froio, Dr. Andrea Zappatore
NEMO group, Dipartimento Energia, Politecnico di Torino, Torino, Italy

Nuclear Engineering MOdeling Group

Introduction

- An unprotected plasma transient event could cause the break of a portion of the BB, leading to an in-vessel LOCA transient
- The pressurized coolant will be released inside the vacuum chamber, giving rise to a flashing jet
- VV failure criterion is local (i.e. pressure peak on gyrotron diamond windows) → need for local analyses in support to global modelling

Aim of the work

- Development of a 3D transient CFD model, able to accurately describe the evolution of the two-phase flashing jet from the moment of the break, up to the opening of the safety Burst Disk (BD)
- Comparison with a 0D model developed with a system-level code
- Comparison with the in-vessel LOCA from a helium-cooled blanket

Assumptions of the model

- The fluid domain is approximated as the plasma chamber
- The divertor region is not considered in order to exploit a double symmetry
- The initial pressure of the vacuum chamber is assumed to be equal to 0.1 bar
- The inlet flow area is lumped in a single, circular region on the OB wall

Mesh adaptivity strategy

An adaptive mesh refinement is employed in order to follow the different shock fronts expected. The adaption is driven by the Mach number variation:

$$\phi = \Delta Ma = \|\nabla Ma\| \cdot \delta \Rightarrow \begin{cases} \phi < 0.1 & \text{Coarsen} \\ 0.1 \leq \phi \leq 0.3 & \text{Keep} \\ \phi > 0.3 & \text{Refine} \end{cases}$$

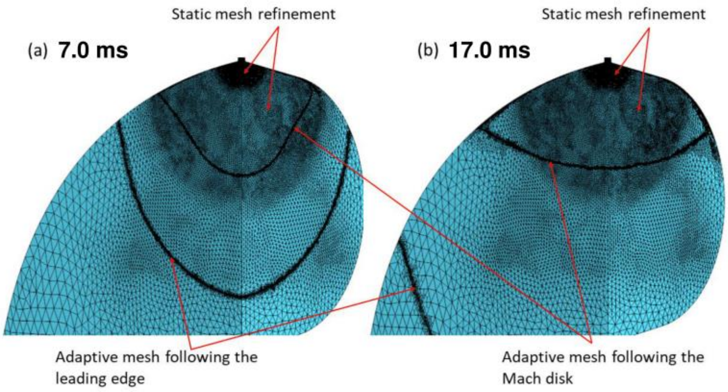

Results

- 2 seconds simulated
- Water initial conditions: 155 bar, 295 − 328°C
- Supersonic jet with $Ma_{MAX} = 1.7$
- Mass flow rate ≅ 650 kg/s

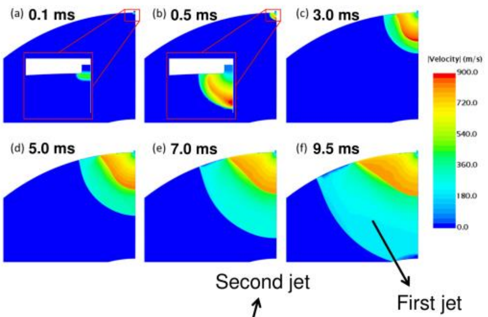

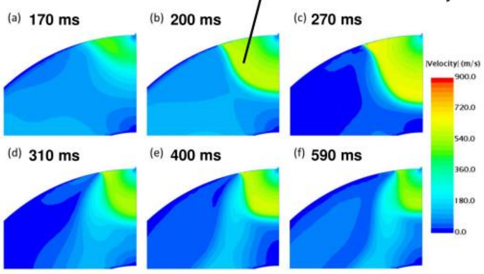

- Reflected pressure wave
- Condensation of the shock front
- Steep pressure peak on the outboard wall (6 bar → 63 bar)

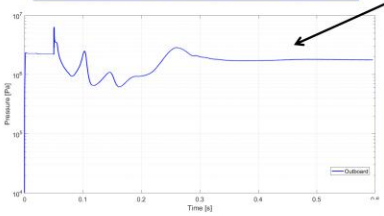

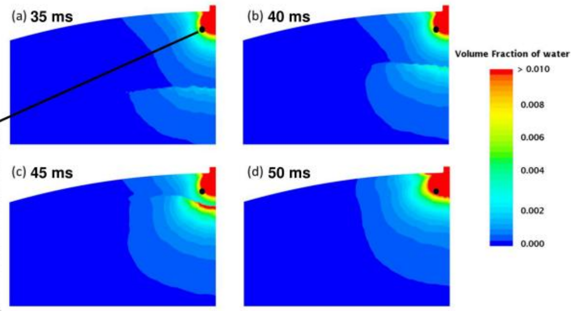

- The wave impact with the BD is relatively weak
- BD pressure follows the average pressure in the chamber
- Opening set-point reached after 2.0 s
- 0D analysis gives conservative results

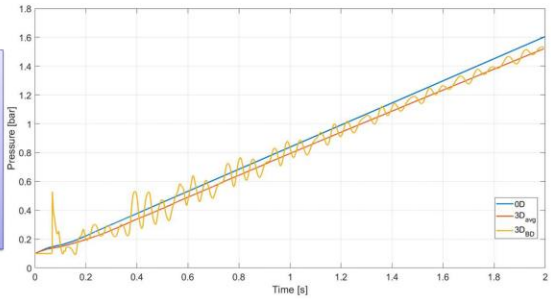

- More energetic
- Transient ends after 57 ms
- 3.5 bar peak on the front wall

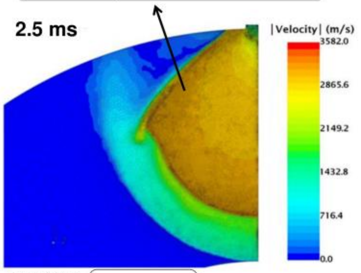

Adapted from [1]

HCPB

- Less energetic
- Transient ends after 2.0 s
- 0.35 bar peak on the front wall

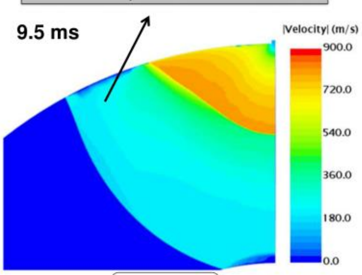

WCLL

Conclusions and perspective

- 3D CFD model of an in-vessel LOCA from a water-cooled BB, developed with the commercial software STAR-CCM+
- Flashing jet evolution modelled from the moment of the break, up to the opening of the safety BD
- The pressure peak on the front wall and the one on the BD surface are much weaker than in the case of a single-phase coolant release
- Reflected pressure wave with condensation of the shock front causes a steep pressure increase on the wall close to the rupture
- 0D model is sufficient as far as the pressure on the BD and the timing for their opening are concerned
- In perspective, some of the model's simplifying assumptions are planned to be addressed

References

[1] Zappatore, A.; Froio, A.; Spagnuolo, G.A.; Zanino, R. 3D transient CFD simulation of an in-vessel loss-of-coolant accident in the EU DEMO fusion reactor. *Nucl. Fusion* **2020**, 60, 126001.

NUCLEAR DAYS
UNIVERSITY OF WEST BOHEMIA
ŠKODA JS
CENEN CZECH NUCLEAR EDUCATION NETWORK
EUROfusion
This work has been carried out within the framework of the EUROfusion Consortium, funded by the European Union via the Euratom Research and Training Programme (Grant Agreement No 101052200 – EUROfusion). Views and opinions expressed are however those of the author(s) only and do not necessarily reflect those of the European Union or the European Commission. Neither the European Union nor the European Commission can be held

FIRE PROTECTION AT NPP

Jan Ullmann

Faculty of electrical engineering, University of west Bohemia

FIRE PROTECTION IS VERY IMPORTANT - Fire is considered a dominant contributor to the total risk of core damage for most facilities. The relativecontribution of events to core damage frequency in one nuclear power plant is 45% due to internal fire (The second most common with a 44%contribution is seismic).

FACULTY OF ELECTRICAL ENGINEERING
UNIVERSITY OF WEST BOHEMIA

FIRE PROTECTION AT NPP

Author: Bc. Jan Ullmann, Poster supervisor: Ing. Mašata

NUCLEAR DAYS

INTRODUCTION TO FIRE PROTECTION

FIRE PROTECTION IS VERY IMPORTANT - Fire is considered a dominant contributor to the total risk of core damage for most facilities. The relative contribution of events to **core damage frequency in one nuclear power plant is 45% due to internal fire** (The second most common with a 44% contribution is seismic).

THE BROWNS FERRY FIRE (MARCH 22, 1975)

This fire plays a significant role in the fire safety of nuclear facilities, until then fundamental rules for fire protection had not been introduced. Cause of the fire was ignition of polyurethane foam used in cable penetrations. Fire propagated through the penetration in the cable spreading room wall, causing major damage in the reactor building. **All of the emergency core cooling systems for the Unit 1 reactor were rendered inoperable and portions of Unit 2. The fire and its aftermath revealed some significant inadequacies in design and procedures related to fires. The fire protection programs we know today are a direct result of this fire and its lessons learned.**

METHODS OF FIRE PROTECTION

historically, two methods have been used for the design of fire protecion systems in NPP

DETERMINISTIC METHOD

One of the prescriptive requirements related to the fire protection requirements for safe shutdown capability. The regulation prescribes that the trains will:

- Have a 3-hour barrier between them
- Have 6.1 m of separation, automatic fire suppression, and fire detection, or
- Have a 1-hour barrier between them, automatic fire suppression, and fire detection

Need to comply with all 3 conditions - sometimes impossible.

PERFORMANCE-BASED METHOD

The risk-informed performance-based approach considers risk insights as well as other factors to better focus attention and resources on design and operational issues according to their importance to safety. **This approach relies on a required outcome rather than requiring a specific process or technique to achieve that outcome. It allows licensees to focus their fire protection activities on the areas of greatest risk.**

The deterministic method required a large amount of money to accomplish 20 feet of separation. Hundreds of exceptions were granted, so a second method was developed that is based mainly on risk probabilities (The vast majority of facilities today use the probabilistic method). (1)

IMPORTANT FUTURE TECHNOLOGIES:

This poster is devoted to **future technologies** (I will introduce you to four technologies) that could be part of fire safety in nuclear facilities. At the moment, we use these systems minimally, but in the future, they could play a significant role in increasing the safety of nuclear power plants.

AI – Machine learning

AI can help **improve fire detection algorithms and reduce false alarms.** By analysing data from different sensors, AI can detect unusual patterns and warn staff of potential problems that could lead to a fire. **They can also assist with strategy during a fire**, significantly increasing the overall efficiency and speed of fire suppression.
Integrating predictive maintenance techniques can help identify potential fire hazards by monitoring the critical condition of equipment. Predictive maintenance can greatly enhance early failure detection and streamline the maintenance process.

01

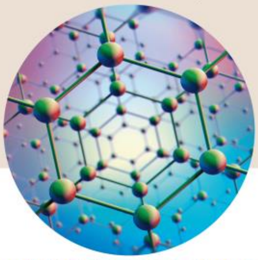

NANOTECHNOLOGY

Nanomaterials can increase **the thermal and mechanical properties of building materials or cables**, making them **more resistant to fire and other extreme conditions.**
However, it should be noted that the development of new materials may also affect the conditions for the emergence and spread of threats, as well as the type of compounds emitted in the environment.
The development of nanotechnology will also influence the development of **flame-retardant electrical cables.**

02

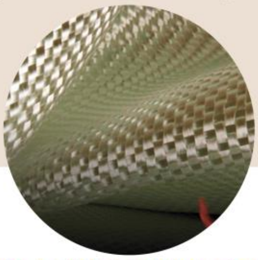

COATING-ISULATION

Insulation and special flame-retardant coatings can greatly advance critical infrastructure in nuclear power plants. **These coatings can delay the spread of fire, which in turn allows personnel to respond more effectively.** When a fire occurs, the temperature of the structures affected by the fire increases and the coating begins to perform its function. The substances involved in eliminating the effects of the fire are activated.
New methods of designing electrical systems can also greatly help with the potential risk of fire due to faults in cable chambers.

03

ROBOTIC SYSTEMS

A robotic firefighting system specifically developed for nuclear facilities **can minimize the potential impact on human lives,** where a robot could replace a human on the front lines fighting a fire. They can be used especially in challenging areas of a nuclear power plant. (2)
These systems are **expanding rapidly thanks to the development of leading robotic manufacturing companies,** i.e. Boston Dynamics. The installation of radiation detectors on robots is being developed at UMASS Lowell. **The development of artificial intelligence and machine learning can greatly help robotic systems in industry**

04

TRAINING IMPACT

The important factor of increasing the level of fire safety is undoubtedly in the technological part, but it is necessary to move in **personnel training and drill.** Coordination of human resources greatly enhances the effectiveness of fire safety. **At the same time, it is very important to focus on following rules and learned procedures, otherwise they will be meaningless.**

CONCLUSION

The most important thing for the implementation of these technologies will be **overcoming the legislative processes** (also the development of these technologies in other fields and ensuring high reliability). Thanks to the development of artificial intelligence, another method for fire protection may be developed. It will be interesting to observe this trend already in the development of small modular reactors.

Historically, **new technologies have always had to prove their safety and profitability in the financial market.** In turn, technology development can **reduce operating and acquisition costs in the future**, making **nuclear power more competitive.**

References

[1] Fire Protection for Operating Reactors. Nuclear Regulatory Commission [online]. March 20, 2020 [cit. 2023-07-26].Available from: https://www.nrc.gov/about-nrc/fire-protection/op-reactors.html
[2] Steven James Hill. The Future is Now: Emerging Technologies in Fire Protection. Total Fire Protection Asia Co.

Contact: ullmann@students.zcu.cz

Ph.d. STUDENTS

METHODS FOR SAFETY AND STABILITY ANALYSIS OF NUCLEAR SYSTEMS

Nicolò Abrate

Energy department - NEMO group Corso Duca degli Abruzzi – 10129, Turin (Italy)

The core design is an iterative process which requires to solve many times the effective multiplication k eigenvalue problem. To speed up iterations, approximations are usually employed.

Methods for safety and stability analysis of nuclear systems

Nicolò Abrate
Politecnico di Torino
Energy department - NEMO group
Corso Duca degli Abruzzi – 10129, Turin (Italy)

Nuclear Days, University of West Boemia, (Pilsen), 14-15 September 2023

Framework and motivations

Nuclear power is a fundamental source of carbon-free energy → Safety is one of the challenges for current and future nuclear power plants → Development of computationally efficient **methods for the safety and stability analysis** of nuclear systems

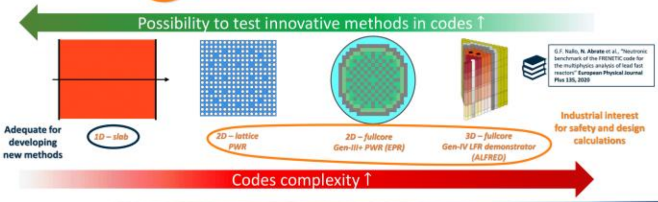

A new eigenvalue formulation for core design

The core design is an iterative process which requires to solve many times the effective multiplication k eigenvalue problem. To speed up iterations, approximations are usually employed

This iterative process can be tackled introducing a density-eigenvalue ζ acting directly on the isotopes whose concentration have to be determined in the design process.

The ζ eigenvalue equation allows estimating the effect of a specific nuclide X and its location in the reactor on the total balance, in a **self-consistent** way.

The main advatanges of ζ are:

- The regions $\mathcal{V}x$ containing X do not need to be adjacent (e.g., control rods)
- ζ is a scaling factor for the atomic density (or concentration) of the isotope X in the region $\mathcal{V}x$
- A physical solution may not exist: in case the steady state cannot be attained acting on the concentration of X in a certain region of the phase space, the design should be changed

The theory of density-eigenvalue ζ allows to determine the density of a certain nuclide to achieve criticality in one iteration, **providing the density correction and the critical flux in one shot (↓)**

An in-house Python package called TEST (Transport Equation Solver in Turin) has been developed from scratch to solve the ζ eigenvalue problem in a slab with finite-difference, P_N, multi-group framework. The code will be freely available on GitHub soon

Examples of practical interest for core design

What is the critical concentration of absorber for the control rods?

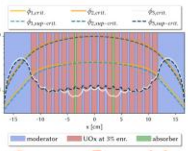

3-group, P_1 model

What is the critical moderation ratio in a LWR?

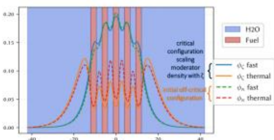

2-group, P_3 model

What is the critical concentration of ^{233}U to be diluted in the Gen-IV molten salt fast reactor design?

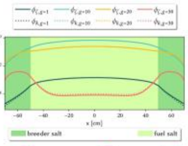

30-group, P_1 model

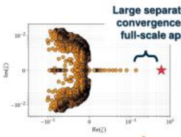

ζ eigenvalue spectrum (↑) for the 30-group, P1 case.
The star is the fundamental eigenvalue, i.e. the physical correction factor that makes the system critical

This new approach can boost the design of:
- ❑Fuel enrichment (e.g. Pu concentration in MOx)
- ❑Chemical shim control (e.g. Boron concentration in water)
- ❑Control rods (e.g. Cd or B density)

Research awarded with the ENEN PhD prize 2022
Best student presentation at PHYSOR 2022

N. Abrate, S. Dulla, P. Ravetto, P. Saracco, *Formulation of the Density Eigenvalue Problem in Neutron Transport for Relevant Engineering Applications*, **Nuclear Science and Engineering**, 2023

My PhD in a nutshell

Non-intrusive reduced order models for parametric safety analyses

Spatial instabilities may arise in the cold start-up phase of large PWRs (e.g., the EPR)

Thermal feedback are less effective

✕ Experimental detection difficulties at low power

Operational issues due to local physical perturbations (e.g., assembly bowing)

✕ Legacy codes are inefficient for such kind of analysis

Study case: 2D model of the NEA Gen-III+ benchmark (UAM)

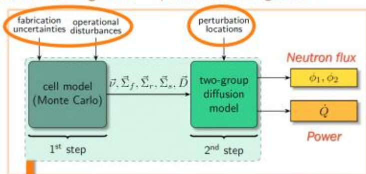

Two-step computational model:
- assembly calculation for group constants (Serpent 2 Monte Carlo code)
- full-core calculation for power (FreeFEM++ model)

Two-step, non-intrusive reduced-order model (NIROM):
- Polynomial Chaos Expansion for assembly calculation
- POD+RBF for full-core, two-group diffusion

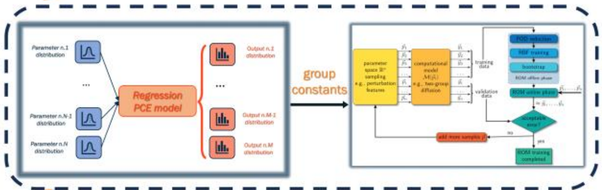

NIROM trained with 1024 samples (64 perturbation spatial arrangements x 16 perturbation magnitudes)

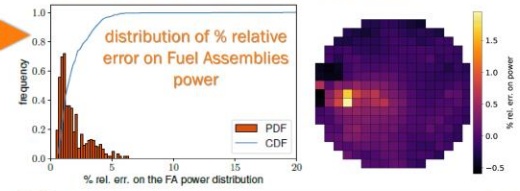

- ~0.3 s (ROM) vs. 960 s (finite element diffusion) for a full-core static calculation
- very good agreement with respect to the full-order model

N. Abrate, S. Dulla, N. Pedroni, *A non-intrusive reduced order model for the characterisation ofthe spatial power distribution in large thermal reactors*, **Annals of Nuclear Energy 184**, 2023

Nuclear data uncertainty propagation for Gen-IV reactors

N. Abrate, A. Aimetta, S. Dulla, N. Pedroni, *Nuclear Data Uncertainty Propagation for the Molten Salt Fast Reactor Design*, **Nuclear Science and Engineering**, 2023

N. Abrate, S. Dulla, P. Ravetto, *Generalized perturbation techniques for uncertainty quantification in lead-cooled fast reactors*, **Annals of Nuclear Energy 164**, 2023

Nuclear data uncertainties

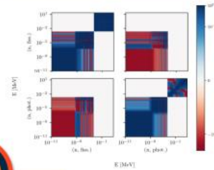

Example of input uncertainty: Pu-239 covariance matrix scored on 1500 energy group (from ERRORR module of NJOY code)

Perturbation and non-intrusive methods for uncertainty quantification

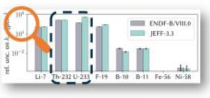

***Very large** uncertainty on k_{eff} for fissile nuclides in the **fuel salt** [pcm] computed with GPT routine in Serpent 2*

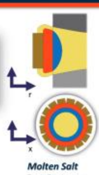

Molten Salt Fast Reactor (EU design)

1/6 of the ALFRED core design (LFR demonstrator)

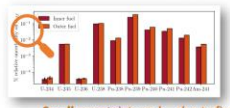

***Small** uncertainty on k_{eff} due to fissile isotopes in **fuel assemblies** [pcm] computed with GPT routine in Serpent 2*

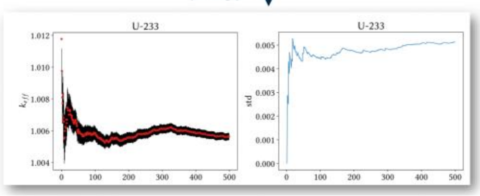

***Large** uncertainty on k_{eff} due to U-233 computed with the Total Monte Carlo approach (using Serpent 2 as a computational model)*

Final remarks

The PhD activity focused on the development of new methods and models, dealing with important issues in reactor physics and reactor design

The work has been always carried out trying to bridge theoretical aspects and practical applications

Contributions have been made in different research fields of fission reactor physics and reactor design

The nuclear data uncertainty propagation pointed out the need for more accurate data evaluations for uncommon isotopes like Th-232 and U-233

GREEN REVOLUTION FOR EUROPE: NUCLEAR ENERGY AS WAY TO SUSTAINABLE DEVELOPMNET AND ENVIRONMENTAL PROTECTION

Alona Bosiuk

Nuclear power i sone of the most efficient and environmentally friendly forms of electricity generation. It fits perfectly into the concept of sustainable development, as it has a low carbon footprint, does not emit harmful gasses, and helps reduce dependence on traditional fossil energy sources. The use of nucelar power can contribute to the creation of an energy-sustainable and environmentally friendly Europe.

Green revolution for Europe: nuclear energy as a way to sustainable development and environmental protection

Abstract

Nuclear power is one of the most efficient and environmentally friendly forms of electricity generation. It fits perfectly into the concept of sustainable development, as it has a low carbon footprint, does not emit harmful gases, and helps reduce dependence on traditional fossil energy sources. The use of nuclear power can contribute to the creation of an energy-sustainable and environmentally friendly Europe.

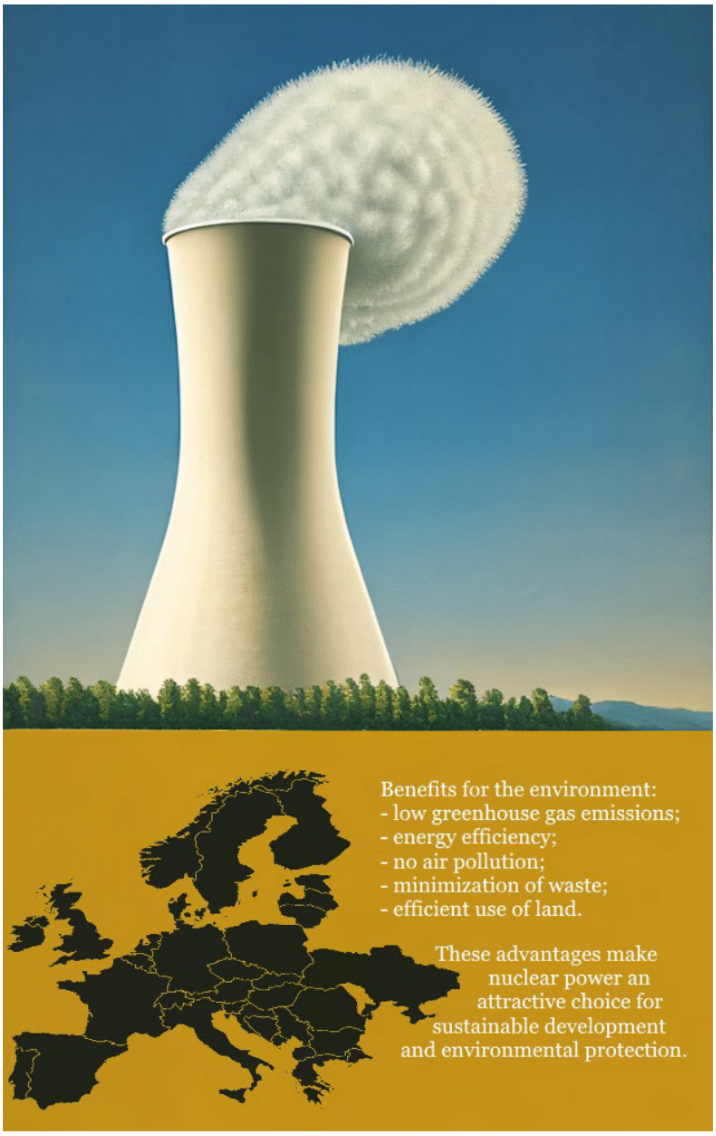

Nuclear power can provide a significant amount of clean electricity, addressing climate change and air pollution, and contribute to the green revolution in Europe.

Main objective:

This poster is dedicated to discussing the potential of nuclear energy as a way to achieve sustainable development and environmental protection in Europe. The purpose of this study is to explore the benefits, challenges and opportunities associated with the use of nuclear energy in the context of the green revolution. The study is aimed at assessing the potential of nuclear energy to ensure sustainable development, reduce greenhouse gas emissions, reduce carbon dependence and preserve the environment.

Conclusion:

Low greenhouse gas emissions contribute to the fight against climate change and provide an energy system that meets environmental requirements. In addition, the energy efficiency of nuclear power plants allows for the efficient use of limited resources and the provision of a significant amount of electricity. Stability of supply is one of the key advantages of nuclear energy, as it ensures independence from external factors and guarantees a continuous supply of electricity.

Alona.Bosiuk@mit.khpi.edu.ua

THE CONSTRUCTION OF SHAKER EXPERIMENTAL FACILITY ANDCHALLENGES AHEAD

Michal Cihlář

Czech Technical University in Prague, FME, Czech Republic

Molten salt reactors (MSRs) has been studied since the 1950s. The research and development of MSRs is gaining a momentum in the past years. However, thermohydraulic experiments with molten salts are challenging due to their time, financial, technical, and organizational demandigness.

One of the ways to avoid such demandigness is to use scaled-down 1,2,3 Such an experimental device working with thermal oil at lower temperatures with similar behavior to molten salts called SHAKER (Scaled down tHermal oil Ardent salt trickle Experimental Research device) is being built in the FFaculty of Mechanical EngineeringCTU in Prague laboratories.

Its main purpose is to verify the possibility of using scaledscaled-down models for the study of molten salt systems.

It aims to advance the field using a combination of this scaled down experimental device, original molten salt experiments references, and CFD models

The Construction of SHAKER Experimental Facility and Challenges Ahead

CTU
CZECH TECHNICAL UNIVERSITY IN PRAGUE

CVŘ | Research Centre Řež

Michal Cihlář[1,2,*]
[1]Czech Technical University in Prague, FME, Technická 4, 160 00 Prague, Czech Republic
[2]Research Centre Řež, Hlavní 130, 250 68 Husinec-Řež, Czech Republic
*Corresponding author: michal.cihlar@cvut.cz

Introduction

Molten salt reactors (MSRs) has been studied since the 1950s. The research and development of MSRs is gaining a momentum in the past years. However, thermohydraulic experiments with molten salts are challenging due to their time, financial, technical, and organizational demandingness.

One of the ways to avoid such demandingness is to use **scaled-down experiments**.[1,2,3] Such an experimental device working with thermal oil at lower temperatures with similar behavior to molten salts called SHAKER (Scaled-down tHermal oil – Ardent salt tricKle Experimental Research device) is being built in the Faculty of Mechanical Engineering CTU in Prague laboratories.

Its main purpose is to verify the possibility of using scaled-down models for the study of molten salt systems.

It aims to advance the field using a combination of this scaled-down experimental device, original molten salt experiments references, and CFD models.

SHAKER Description

The comparison of properties for real experiments and SHAKER is given in Table 1. The SHAKER is designed to simulate the behaviour of FLiBe salt at 700 °C and solar salt at 300 °C. Therefore, Therminol D12 therma oil was chosen as the working fluid. The properties of Therminol D12 at 65 °C are presented in Table 2.

SHAKER (Figures 1, 2) is made out of AISI 316L stainless steel pipes with dimensions of D30x3, heigth of 1,5 m, and length of 2,0 m. The pipes are heated by electric resistive heating and covered with the EPDM (ethylene propylene diene monomer rubber) synthetic rubber heat insulation.

Table 1: Comparison of real and scaled-down experiments

Experiment	Temperature	Working Fluid	Mean Velocity	Inner Diameter	Time Scale	Temperature Scale	Wall Thickness
	[°C]	[-]	[cm/s]	[mm]	[-]	[°C]	[mm]
FLiBe real	700	LiF-BeF$_2$	4.0	54	1	1	4.75
FLiBe model	65	Therminol D12	2.6	24	0.675	0.18	3.0
Solar salt real	300	NaNO$_3$-KNO$_3$	4.0	50	1	1	3.5
Solar salt model	105	Therminol D12	2.8	24	0.7	0.05	3.0

Challanges Ahead

During the FLiBe model operation SHAKER is planned to work with 45 °C on the cold leg and 85 °C on the hot leg. The expected Therminol D12 velocities ranges from 1 cm/s to 10 cm/s and mass flow rates are about 5-15 g/s.

Such small velocities and flowrates are hard to measure. Especially, in the environment of natural circulation, where any additional pressure losses are to be avoided.

Therefore, a combination of ultrasonic flowmeters, invasive flowmeters (float or paddle), and calorimetric flowmeters will be employed.

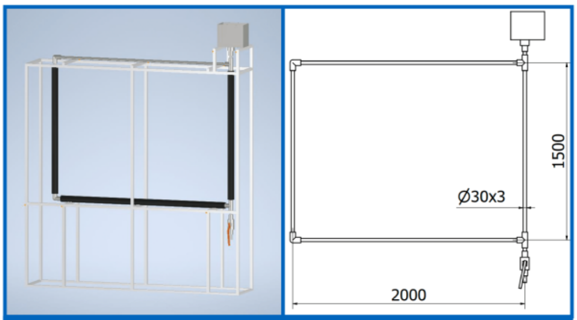

Figure 1: SHAKER visualization and main dimensions

Conclusion

- SHAKER – scaled down experimental device for the study of molten salts' natural flow is under construction
- SHAKER will simulate behavior of FLiBe salt at 700 °C and solar salt at 300 °C
- The flow measurement will be the most challenging part


Figure 2: SHAKER experimental device under construction

Acknowledgement

This work was supported by the Grant Agency of the Czech Technical University in Prague, grant No. SGS22/102/OHK2/2T/12

Table 2: Therminol D12 properties at temperature of 65 °C[4]

Parameter	ρ	c_p	$\rho \cdot c_p$	ν	λ	β
Unit	kg·m^{-3}	kJ·kg^{-1}·K^{-1}	kJ·m^{-3}·K^{-1}	m^2·s^{-1}	W·m^{-1}·K^{-1}	K^{-1}
Value	703.2	2.414	1698	5.90·10^{-7}	0.0966	0.0011

References

[1] Aksan (2019). An overview on thermal-hydraulic phenomena for water cooled nuclear reactors; part I: SETs, and ITFs of PWRs, BWRs, VVERs. Nuclear Engineering and Design Volume 354. DOI: 10.1016/j.nucengdes.2019.110212
[2] Zweibaum et al. (2020). Scaling Methodology for Integral Effects Tests in Support of Fluoride Salt–Cooled High-Temperature Reactor Technology. Nuclear Science and Engineering, 194(8-9). DOI: 10.1080/00295639.2019.1710976
[3] Bardet & Peterson (2008). Options for Scaled Experiments for High Temperature Liquid Salt and Helium Fluid Mechanics and Convective Heat Transfer. Nuclear Technoogy, 163(3). DOI: 10.13182/NT163-344
[4] SOLUTIA (n.d.). Therminol D12: Datasheet. Dostupné z: http://twt.mpei.ac.ru/TTHB/HEDH/HTF-D12.PDF

Take a picture for more information

linktr.ee/michal.cihlar

JADERNÉ DNY 2023
14.–15.9.2023

DESIGN AND THERMAL-HYDRAULIC TRANSIENT ANALYSIS OF PRIMARY COOLING SYSTEMS FOR TOKAMAK FUSION REACTORS

Cristiano Ciurluini

Sapienza University of Rome

My Ph.D. was conducted in the frame of the EUROfusion Consortium research activity, within a collaboration between DIAEE of Sapienza University of Rome and the Experimental Engineering Division of ENEA (Brasimone R.C.). Since mid-2017, I have been working in the research team associated toWork Packages Breeding Blanket (BB) and Balance of Plant (BoP).

Design and thermal-hydraulic transient analysis of primary cooling systems for tokamak fusion reactors

Ph.D. in Energy and Environment at Sapienza University of Rome, XXXIV ciclo, 2018-2021

Ph.D. Thesis defended on 14th February 2022

Candidate: **C. Ciurluini**; Thesis Advisor: Prof. F. Giannetti; Co-Supervisors: Prof. G. Caruso, Ing. A. Del Nevo, Ing. A. Tincani

Activity Framework

My Ph.D. was conducted in the frame of the **EUROfusion Consortium** research activity, within a collaboration between **DIAEE of Sapienza University of Rome** and the **Experimental Engineering Division of ENEA (Brasimone R.C.)**. Since mid-2017, I have been working in the research team associated to **Work Packages Breeding Blanket (BB)** and **Balance of Plant (BoP)**.

Goal: The research activity was focused on the **conceptualization** and **thermal-hydraulic assessment** of the **cooling system** for the **Water-Cooled Lead-Lithium (WCLL) blanket option**, involving **ITER** and **DEMO** fusion reactors.

Main Topics: Fusion reactor design; Thermal-hydraulics; System codes; Transient analysis; Control systems; Management strategy for accident mitigation.

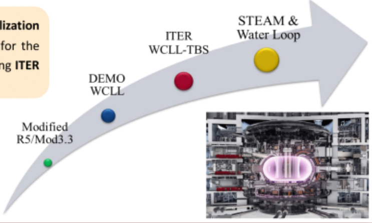

Modified R5/Mod3.3

During the Ph.D., I became a proficient user of RELAP5/Mod3.3, a fully validated system code to perform transient analysis. Since it missed some features to properly model the fusion power plants, I collaborated to the development, the verification and the preliminary validation of a modified version of the code, more suitable for fusion reactor design.

Workflow

1. **Plant Description** (CAD, PFD, P&ID, isometric view)
2. **Engineering Handbook Definition**
3. **Input deck preparation**: Nodalization (control volumes, junctions, heat structures); Control system; Boundary/Initial conditions.
4. **Post-processing and result analysis** (MATLAB)

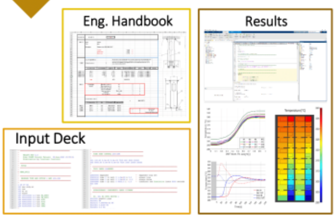

Code Modifications

1. **Lead-lithium** and **HITEC©** working fluids, with their thermophysical properties (EUROfusion database)
2. **New heat transfer correlations** for added working fluids (Seban-Shimazaki, Cheng-Tak, Ushakov, Mikityuk, Kazimi-Carelli, Graber-Rieger, Sieder-Tate,)
3. **Helicoidally tubes** heat transfer correlations (Mori-Nakayama and Zukauskas) and dedicated dry-out point (thermal crisis) control loop

VERIFICATION: Simple Thermal-Hydraulics problems were run to verify the effectiveness of features implemented in the code.

VALIDATION: Comparison among simulation results and experimental data coming from facilities where heat transfer phenomena were tested.

What is a Breeding Blanket?

In a fusion power plant, the BB is a key reactor component, accomplishing several functions: **cooling device**, **tritium breeder** and **neutron shield**. In a top-down scheme, it is divided n **sectors**, **segments** and **breeding cells** (system elementary units). It is composed of two principal subsystems: the **first wall (FW)** and the **breeding zone (BZ)**, each one provided with an independent cooling circuit. My research activity focused on these systems.

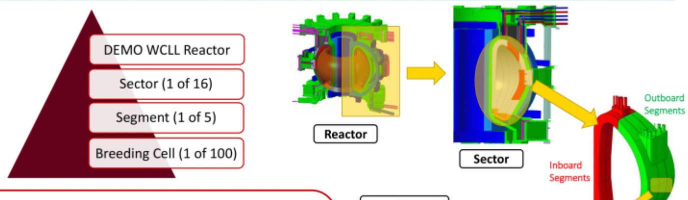

WCLL BB relies on:

- Ferritic-martensitic steel (EUROFER-97) as structural material, because of its reduced activation;
- Liquid lead-lithium enriched at 90% in Li^6 as breeder, neutron multiplier and tritium carrier;
- Pressurized water as coolant (295–328 °C and 15.5 MPa).
- A tungsten layer to cover the plasma facing surface.

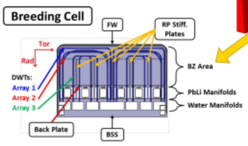

BB cooling system design approach

The design process was articulated in several steps. Starting from the **system requirements** and **boundary conditions**, a **preliminary layout** was defined, together with the **sizing of all the main circuit components**. **Transient analysis** was then used to refine and improve the project. Indeed, it allows to fully characterize the **system performances** not only in **nominal conditions** but also in a wide range of **operational and accidental scenarios**.

Numerical simulations make also possible to **test and tune control systems and accidental management strategies** able to keep the circuits in safe conditions in all considered transient evolutions.

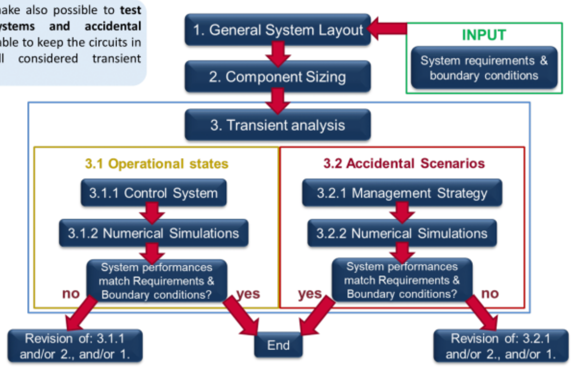

Ph.D. Thesis Outcomes

The above approach was successfully applied to the **WCLL technology** considering both **ITER** and **DEMO reactors**. The design activity proved to be quite challenging since the system layout was strongly driven by the peculiarities of a nuclear fusion reactor, first the **pulsed plasma regime** characterizing its normal operations. The design rationale was adopting well proven nuclear equipment, such as the one already used for PWRs, by developing innovative solution for the circuit layout, adapting the component sizing to the fusion environment, and demonstrating its suitability for the new working conditions. Finally, the **transient analysis** demonstrated the appropriateness of the developed design when withstanding a wide range of selected operational and accidental scenarios.

DEMO WCLL BB Primary Heat Transfer System

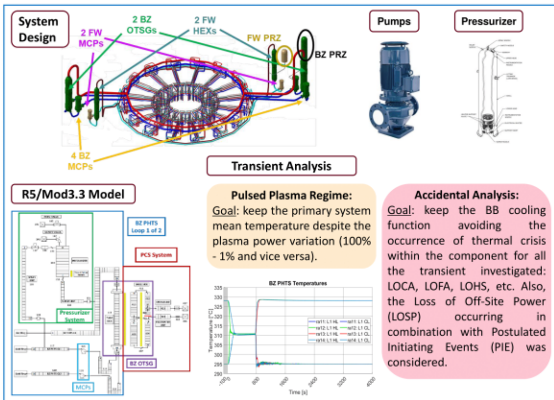

Pulsed Plasma Regime: Goal: keep the primary system mean temperature despite the plasma power variation (100% - 1% and vice versa).

Accidental Analysis: Goal: keep the BB cooling function avoiding the occurrence of thermal crisis within the component for all the transient investigated: LOCA, LOFA, LOHS, etc. Also, the Loss of Off-Site Power (LOSP) occurring in combination with Postulated Initiating Events (PIE) was considered.

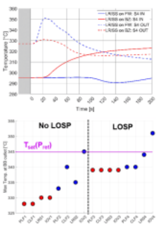

ITER WCLL Test Blanket Module Water Cooling System

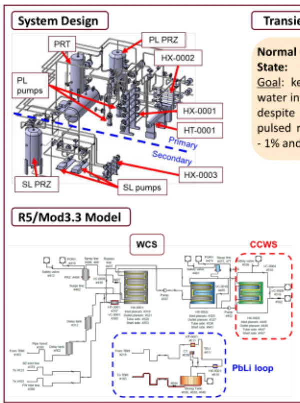

Transient Analysis

Normal Operation State: Goal: keep the TBM water inlet conditions despite the plasma pulsed regime (100% - 1% and vice versa).

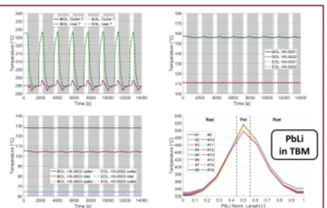

Accidental Analysis: Goal: Demonstrate that WCS control system can keep the TBM cooling function for a plasma pulse (no triggering of Fast Plasma Shutdown System), i.e., a minor WCS accident does not interfere with ITER global operation.

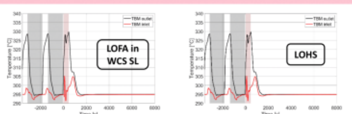

This work has been carried out within the framework of the EUROfusion Consortium, funded by the European Union via the Euratom Research and Training Programme (Grant Agreement No 101052200 — EUROfusion). Views and opinions expressed are however those of the author(s) only and do not necessarily reflect those of the European Union or the European Commission. Neither the European Union nor the European Commission can be held responsible for them.

DESIGN OF EXPERIMENTAL METHODS FOR INVESTIGATING CORIUM PROPERTIES AND BEHAVIOR

Jan Hrbek

Faculty of Electrical Engineering, University of West Bohemia, Pilsen, Czech Republic

New methods are needed to study molten core (corium) properties and behavior, as the Fukushima I accident demonstrated the importance of understanding core meltdowns. The work focuses on method determining density of molten high-temperature material. Current experimental methods based on levitation and shape analysis have limitations, so presented research aims to develop a method based on different physical principles. The new method will enhance nuclear power plant safety by providing crucial data to describe processes during accidents.

Design of Experimental Methods for Investigating Corium Properties and Behavior

www.cvrez.cz

Jan Hrbek [a,b]
jan.hrbek@cvrez.cz
[a] *Faculty of Electrical Engineering, University of West Bohemia, Pilsen, Czech Republic*
[b] *Research Centre Rez, Husinec-Rez, Czech Republic*

Introduction and motivation:

New methods are needed to study molten core (corium) properties and behavior, as the Fukushima I accident demonstrated the importance of understanding core meltdowns. The work focuses on method determining density of molten high-temperature material. Current experimental methods based on levitation and shape analysis have limitations, so presented research aims to develop a method based on different physical principles. The new method will enhance nuclear power plant safety by providing crucial data to describe processes during accidents.

Method:

The proposed method uses induction melting in a cold crucible to reach high temperature and prevent melt contamination. The cold crucible walls and bottom are intensively water-cooled; thus, the sample is not melted in the contact area with the cold crucible and thin solid state layer is formed. This solid-state layer is called the skull. The induction melting in the cold crucible allows to reach temperature up to 3200 °C.

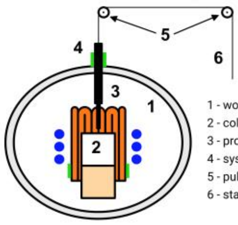

1 - working chamber
2 - cold crucible with melt and inductor
3 - probe
4 - system of bearings and probe holder
5 - pulleys
6 - stainless steel rope

A new method involves melting the sample material, describing the melt's geometry, and calculating its density. A specialized device immerses a stainless steel probe in the melt for 2 seconds, forming an oxide layer on the probe's surface. After the experiment, each probe is photographed twice and processed using self-made software to measure the distance in pixels, with pixel size calibrated for each image [1].

The volume of the melt is obtained from

$$V_{\mathrm{melt}} = \frac{\pi \cdot \left(d_{\mathrm{ing}} - 2 \cdot d_{\mathrm{wskull}}\right)^2}{4} \cdot h_{\mathrm{melt}} - \frac{\pi \cdot d_{\mathrm{probe}}^2}{4} \cdot h_{\mathrm{melt}}$$

where d_{ing}—diameter of the ingot, d_{wskull}—thickness of the skull in the wall of the cold crucible, h_{melt}—height of the melt, d_{probe}—diameter of the measuring stainless steel probe. Skull layer thickness was measured using a calibrated optical microscope. To enhance visibility, Cr_2O_3 was added to the melt before the experiment's last phase. The addition turned the melt purple upon solidification, while the skull remained white because the skull remained solid for the whole time. This improved contrast for skull thickness analysis.

$$V_{\mathrm{skull}} = S_{\mathrm{ing}} \cdot \left(h_{\mathrm{melt}} + d_{\mathrm{bskull}}\right) - V_{\mathrm{melt}}$$

where V_{skull}—volume of the skull layer, S_{ing}—cross section of the ingot, h_{melt}—height of the melt, d_{bskull}—thickness of the skull layer on the bottom of the cold crucible, V_{melt}—volume of the melt.

$$m_{\mathrm{melt}} = m_{\mathrm{ing}} - V_{\mathrm{skull}} \cdot \rho_{\mathrm{skull}}$$

where m_{melt}—mass of the melt, m_{ing}—mass of the ingot, V_{skull}— volume of the skull layer, ρ_{skull}—density of the skull layer. The density of the skull layer was measured using the pycnometric method after the experiment.

The melt density is obtained from

$$\rho_{\mathrm{melt}} = \frac{m_{\mathrm{melt}}}{V_{\mathrm{melt}}}$$

Induction system with cold crucible; 1 – inductor, 2 – cold crucible, 3 – moving device

The measuring stainless steel probe after interaction with the melt

Thickness of the skull layer – white color = skull layer, purple color = solidified melt colored using Cr_2O_3

Experimental verification:

The proposed method was tested using non-radioactive corium simulants: Z50 (50 wt. % ZrO_2 + 50 wt. % Al_2O_3), Z60 (60 wt. % ZrO_2 + 40 wt. % Al_2O_3), and Z80 (80 wt. % ZrO_2 + 20 wt. % Al_2O_3). We developed a new method to measure the liquidus and solidus temperatures of high-temperature melts for these simulants to define temperature ranges for verification of the density measurement method. The temperature ranges for density measurement were:

Z50: 2100 °C – 2400 °C (measured liquidus temperature = 1940.2 °C)
Z60: 2100 °C – 2400 °C (measured liquidus temperature = 2003.2 °C)
Z80: 2400 °C – 2600 °C (measured liquidus temperature = 2255.6 °C)

Density was measured six times for each mixture at different temperatures, and the uncertainty of the measurements was considered. The least squares method was used for data approximation. The Z50 mixture showed good agreement with literature data. For the Z60 mixture, the least squares method was not used due to a significant density drop between 2200°C and 2300°C. The proposed method revealed the density decrease, likely caused by sample instability preventing further measurements at higher temperatures by conventional methods. The Z80 mixture's temperature intervals did not overlap with the reference data.

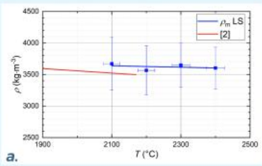

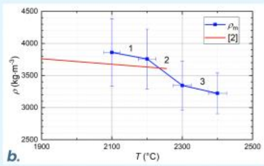

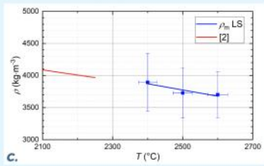

Temperature dependences of mixtures density – Z50 (a), Z60 (b), and Z80 (c) with marked ranges determines the real value of the density lies in the range with a probability *P* = 95 %.

Application:

The proposed method is currently used to obtain Temelin Nuclear Power Plant (NPP) prototypic corium data for the hypothetic Station Black-Out (SBO) scenario to improve the accuracy of severe accident calculations. Current research in this field is carried out within the project TK03020149 supported by TA CR involving UJV Rez and CEZ.

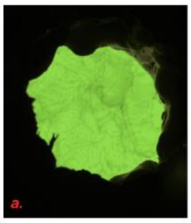

Molten (a) and solidified (b) prototypic corium with a composition corresponding to the hypotetical SBO scenario of accident in the Temelin NPP during (a)/after (b) experiment focused on determination of its density.

Conclusion:

The research was aimed to design and verify the method of density measurement at high temperature for determining corium density. The results are in good agreement with previously measured data by diffrent method (difference less than 5 %). The expanded uncertainty of the measurement does not exceed 14 %. The coverage factor is considered to be *k*=2 and determines the real value of the measured quantity lies in the range with a probability *P*=95 %.

The method proved to be sufficiently accurate to be used to measure the density of corium.

Reference:

[1] Hrbek, J., Mészáros, B., Paukov, M., & Kudláč, M. (2021). Methodology for measurement of density of liquid oxides. *Journal of Nuclear Engineering and Radiation Science*, 7(2), 021601-1-021601–021609. https://doi.org/10.1115/1.4048478

[2] Grishchenko, D.; Piluso, P. (2011). Recent progress in the Gas-Film Levitation as a method for thermophysical properties measurements: application to ZrO2-Al2O3 system. *High Temperatures-High Pressures*, 40 (2), ISSN 0018-1544.

Acknowledgement:

The presented results have been financially supported by the Technology Agency of the Czech Republic (TA CR) - the project TK03020149.

EXPERIMENTAL AND NUMERICAL STUDY OF RING COMPRESSION TEST

Vojtěch Smolíka, Alžběta Endrychováa, Jakub Krejčí

Faculty of Electrical Engineering, University of West Bohemia, Pilsen, Czech Republic

This work focused on simulation of Ring Compression Test (RCT) to evaluate the stress-strain behaviour and hoop fracture properties of Zr-based alloy with 1% of niobium (Zr1Nb), which is widely used as fuel cladding in light water nuclear reactors. The static structural numerical analysis has been performed using ANSYS Mechanical 2023 R1, to evaluate the mechanical properties of experimentally tested samples.and evalua

Experimental and numerical study of Ring Compression Test

Vojtěch Smolík[a,*], Alžběta Endrychová[a,b], Jakub Krejčí[b]

[a]Czech Technical University in Prague, FME, Technicka 4, 160 00 Praha 6, Czech Republic
[b]UJP PRAHA a.s., Nad Kamínkou 1345, 156 00 Praha-Zbraslav, Czech Republic
*Corresponding author: Vojtech.Smolik@fs.cvut.cz

Introduction

This work focused on simulation of **Ring Compression Test (RCT)** to evaluate the stress-strain behaviour and hoop fracture properties of Zr-based alloy with 1% of niobium (Zr1Nb), which is widely used as **fuel cladding** in light water nuclear reactors. The static structural numerical analysis has been performed using **ANSYS Mechanical 2023 R1**, to evaluate the mechanical properties of experimentally tested samples.

Fuel Cladding

Fuel cladding is the **first protective barrier against lost of fission products** which have to withstand extreme conditions from normal operation to intermittent and final dry storage. This hostile environement results in mechanical and microstructural damage of cladding caused by different stress levels, temperature, corrosion, hydrogen pick up and others degradation processes further enhanced by radiation. Because of this, the integrity of cladding is a critical issue.

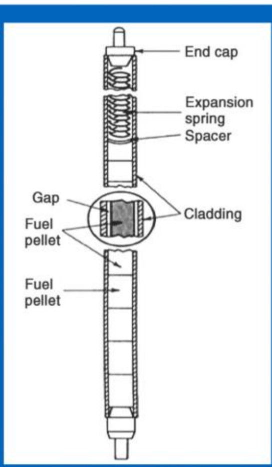

Figure 1: Schematic of LWR fuel rod [1].

Objectives

1. Simulation of **stress-strain behavior** of Zr1Nb fuel cladding at different temperatures.
2. Determination of the tensile and compressive area distribution, Young modulus and yield strength of the speciment.
3. Preparation of simulation of stress-strain behavior and hoop fracture properties of Zr1Nb with different coatings which is considered as **future ATF clladding**.

Numerical simulation

Numerical solution was performed in **ANSYS Mechanical 2023 R1** static structural analysis. The simulation was done up to a deformation of 2 mm, because at this deformation it is already possible to observe if the sample is sufficiently ductile or brittle. **Bilinear isotropic hardening model** was applied to define the material properties of tested sample. The test sample displacement velocity was set to match performed experiment. The sensitivity analysis of used numerical mesh has been performed. Numerical solver has been set to program controlled time step, the duration of experiment is 240 s.

Results

Table 1 shows the parameters of the experimental samples used and the temperature at which the RCT was performed. In ***Figure 2*** it can be seen a comparison of numerical and experimental results of fuel cladding samples at two different temperatures. The numerical resuls perform a lower force reaction than experimental values for both test samples. **The normal tensile** (red) and **compressive** (blue) stress distribution is shown in ***Figure 3*** and in more detail in ***Figure 4***. Contours of **von-Mises stress** of the tested sample are shown in the ***Figure 5***. The stress distribution in the numerical simulation is in agreement with observed crack mechanics of fuel cladding samples.

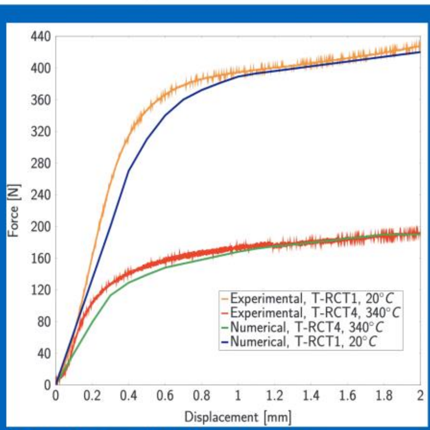

Figure 2: Force-displacement curves - Experimental and numerical results.

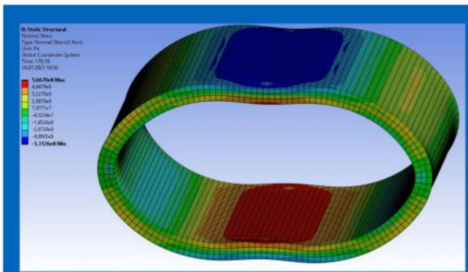

Figure 3: Numerical analysis - distribution of tensile and compressive stress, 2mm displacement, T-RCT1, 20°C

Table 1: Experimental samples properties

Name of sample	T [°C]	l [mm]	h [mm]	t [mm]
T-RCT1	20	10.09	9.10	0.57
T-RCT4	340	10.07	9.11	0.57

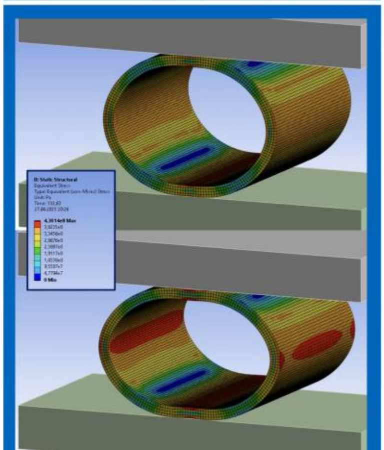

Figure 5: von-Mises stress contour result of numericalsimulation, T-RCT1 sample, 1 mm displacement (up) and 2 mm displacement (down).

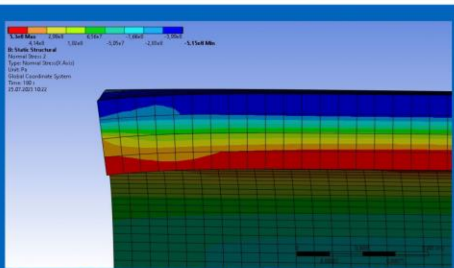

Figure 4: Numerical analysis - detailed distribution of tensile and compressive stress, 2mm displacement, T-RCT1, 20°C

Conclusion

- The RCT is important and simple method used for determination of mechanical properties in hoop direction which is essential for integration of fuel cladding.
- The collapse load and ultimate tensile strenght was determined from load-displacements curves.
- The yield stenght and young modulus for 20°C and 340°C was determined using iterration method.
- The aim of future work is to simulate and determine stress-strain behavior and hoop fracture properties of Zr1Nb with different thin coatings.

References

[1] Allen, Todd & Busby, Jeremy & Meyer, Mitchell & Petti, David. (2010). Materials Challenges for Nuclear Systems. Materials Today - MATER TODAY. 13. 10.1016/S1369-7021(10)70220-0.
[2] Y. T. Reddy and S. R. Reid. On obtaining material properties from the ring compression test. (52):257–263, 1979.
[3] W. G. Luscher, K. J. Geelhood. Material property correlations: Comparisons between frapcon-3.4, fraptran 1.4, and matpro (1), 2010. https://doi.org/10.2172/103089

ACKNOWLEDGMENT

This event has been supported by the Student Scientific Conference 2022 (SVK project) "*Conference of Nuclear days 2022"* of the University of West Bohemia in Pilsen. Project number is SVK1-2022-003.